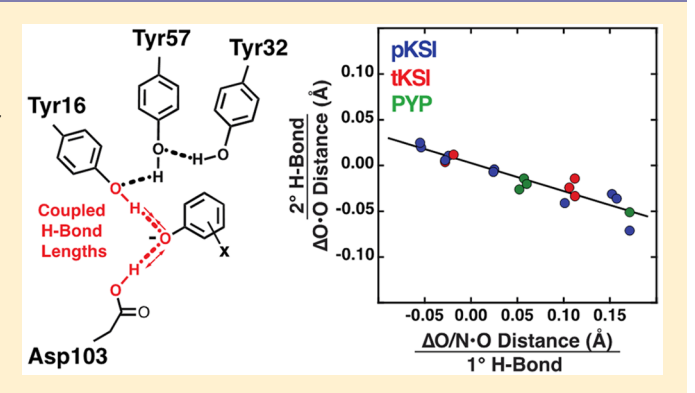


# Structural Coupling Throughout the Active Site Hydrogen Bond Networks of Ketosteroid Isomerase and Photoactive Yellow Protein

Margaux M. Pinney,<sup>†</sup> Aditya Natarajan,<sup>†</sup> Filip Yabukarski,<sup>†</sup> David M. Sanchez,<sup>‡,⊥</sup> Fang Liu,<sup>‡,¶,⊥</sup> Ruibin Liang,<sup>‡,⊥</sup> Tzanko Doukov, Jason P. Schwans,<sup>†,∇</sup> Todd J. Martinez,<sup>‡,⊥</sup> and Daniel Herschlag\*,†,‡,#,§®

Supporting Information

ABSTRACT: Hydrogen bonds are fundamental to biological systems and are regularly found in networks implicated in folding, molecular recognition, catalysis, and allostery. Given their ubiquity, we asked the fundamental questions of whether, and to what extent, hydrogen bonds within networks are structurally coupled. To address these questions, we turned to three protein systems, two variants of ketosteroid isomerase and one of photoactive yellow protein. We perturbed their hydrogen bond networks via a combination of site-directed mutagenesis and unnatural amino acid substitution, and we used <sup>1</sup>H NMR and high-resolution Xray crystallography to determine the effects of these perturbations on the lengths of the two oxyanion hole



hydrogen bonds that are donated to negatively charged transition state analogs. Perturbations that lengthened or shortened one of the oxyanion hole hydrogen bonds had the opposite effect on the other. The oxyanion hole hydrogen bonds were also affected by distal hydrogen bonds in the network, with smaller perturbations for more remote hydrogen bonds. Across 19 measurements in three systems, the length change in one oxyanion hole hydrogen bond was propagated to the other, by a factor of  $-0.30 \pm 0.03$ . This common effect suggests that hydrogen bond coupling is minimally influenced by the remaining protein scaffold. The observed coupling is reproduced by molecular mechanics and quantum mechanics/molecular mechanics (QM/ MM) calculations for changes to a proximal oxyanion hole hydrogen bond. However, effects from distal hydrogen bonds are reproduced only by QM/MM, suggesting the importance of polarization in hydrogen bond coupling. These results deepen our understanding of hydrogen bonds and their networks, providing strong evidence for long-range coupling and for the extent of this coupling. We provide a broadly predictive quantitative relationship that can be applied to and can be further tested in new systems.

# INTRODUCTION

Hydrogen bonds lie at the core of biological function and specificity, as anticipated by Linus Pauling when he coined the term "hydrogen bond" in 1931. 1,2 Hydrogen bonds in proteins are typically found in networks that are readily visualized in high-resolution X-ray structures and play integral roles in protein folding, molecular recognition, catalysis, and allostery.<sup>3–15</sup> Their perceived importance aligns with the difficulties observed in engineering new enzymes, where limitations in the ability to incorporate hydrogen bond networks have been suggested as a key missing feature responsible for the large discrepancy in rate enhancements between natural and designed enzymes. 16-21

It is clear that enzymes greatly restrict dynamics, positioning active site groups that carry out direct catalytic roles, 22-24 and

hydrogen bonds can provide greater positional restraints than individual hydrophobic interactions. 3,25,26 Molten globules, which exist as on- or off-pathway folding intermediates and have a compact yet mobile hydrophobic core, may epitomize the difficulty of specifying a distinct conformational state predominantly via hydrophobic interactions alone. 27-29 Nevertheless, motions remain in proteins even with hydrogen bond networks, most fundamentally because motion is present in every atomic system above 0 K. Furthermore, in proteins, the use of hydrogen bonding and hydrophobic interactions to form secondary and tertiary interactions, rather than covalent bonds, accentuates conformational plasticity. Thus, atomic motions

Received: February 8, 2018 Published: July 10, 2018



<sup>†</sup>Department of Biochemistry, <sup>‡</sup>Department of Chemistry, <sup>#</sup>Department of Chemical Engineering, <sup>§</sup>Stanford ChEM-H, Stanford University, Stanford, California 94305, United States

 $<sup>^{\</sup>parallel}$ Stanford Synchrotron Radiation Light Source and  $^{\perp}$ Department of Photon Sciences, SLAC National Accelerator Laboratory, Menlo Park, California 94025, United States

are pervasive, even in enzymes that do not have explicit conformational changes required for function, such as motor proteins and molecular pumps, and do not require a loop closure or domain motion to align catalytic groups or allow substrate and product ingress and egress.

Indeed, there has recently been much discussion, and speculation, regarding the role of dynamics, or conformational fluctuations, in enzyme function. 30-37 Klinman, through detailed study of tunneling in enzymatic reactions, has provided compelling evidence for conformational rearrangements required to achieve tunneling-competent states.<sup>3</sup> Generalizing from those studies, she has suggested that the most stable, or probable, enzyme-substrate conformation may not be the state that is most catalytically active, as chemical transformations involve the close approximation of atoms, with distances closer than the sum of van der Waals radii, to allow new bonds to form. 30,31,39,44 More speculatively, Klinman has suggested that hydrogen bond networks may provide specially adapted conduits that couple energy transfer from solvent to active sites. 45 Alternative models for the prevalence of hydrogen bond networks include the large energetic cost of leaving unfulfilled buried hydrogen bond donors and acceptors, such that second and third shell hydrogen bonds may be key in stabilizing folded proteins, as well as in positioning active site groups.46 Rearrangements in hydrogen bond networks also occur in many allosteric and regulatory processes, e.g., refs 47-49. Here, we address coupling within hydrogen bond networks in an effort to provide basic information about the conformational interrelationships between hydrogen bonds within protein hydrogen bond networks. This information will be needed to ultimately define and understand the local and collective motions and the extent of conformational restriction within proteins.5

As expected, given their prevalence and importance, there have been many studies and proposals concerning the physical nature and energetic properties of hydrogen bonds (e.g., refs 3, 6, 51–56). Over the past few decades, the notions that shorter hydrogen bonds are stronger and that hydrogen bonds shorten within protein environments to provide additional, and perhaps enormous, energetic contributions to catalysis, has dominated discussions. However, Sigala et al. demonstrated that hydrogen bonds do not shorten in hydrophobic solvents, relative to their lengths in aqueous solution, removing the foundational principle of environment-dependent hydrogen bond shortening that governs this set of proposals. To

Sigala et al. also described a strong correlation between O·O hydrogen bond length, collated from small-molecule neutron diffraction structures, and the difference in aqueous  $pK_a$  values between the hydrogen bond donor and acceptor ( $\Delta p K_a$ ), a relationship that has been discussed extensively (e.g., refs 59, 71-76) and is now expected to hold across different solvent environments (Figure 1A,B). 68,77-79 This general correlation greatly simplifies our consideration of hydrogen bond structure and accounts for ~86% of the variance in hydrogen bond lengths. Nevertheless, the remaining deviations are well beyond the error of small-molecule diffraction data. These deviations are particularly clear from consideration of different crystals of the same compound. To illustrate, we compiled O-O hydrogen bond lengths from 36 high-quality structures of 3,5-dinitrosalicylate in the Cambridge Structural Database.<sup>80</sup> Variations on the order of a tenth of an Ångstrøm were observed, well beyond coordinate errors for small molecule

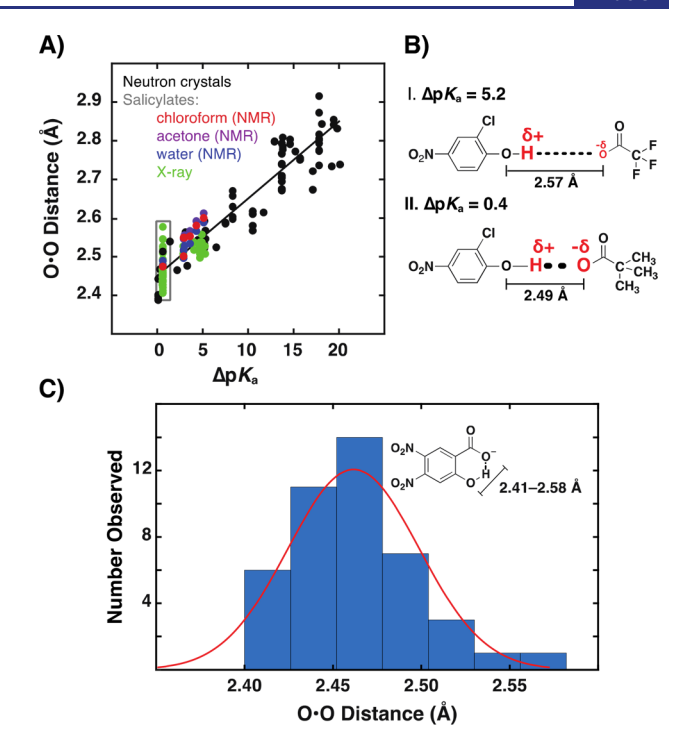


Figure 1. Hydrogen bond lengths display a strong dependence on donor-acceptor  $\Delta p K_a$ . (A) Hydrogen bond lengths correlate with donor-acceptor  $\Delta p K_a$  with a slope of 0.020 Å/p $K_a$  ( $R^2 = 0.86$ , i.e., the model describes 86% of the variation in the data) for a series of inter- and intramolecular hydrogen bonded complexes with donoracceptor pairs covering a range of 20  $\Delta p K_a$  units. Points representing 3,5-dinitrosalicylate from X-ray, neutron, and NMR are boxed and plotted in (C). Here,  $\Delta p K_a$  values are calculated as the difference in  $pK_a$  of the hydrogen bond donor and the conjugate acid of the acceptor in water. (B) As hydrogen bond donor-acceptor  $\Delta p K_a$  approaches zero, the partial charges on the donor and acceptor molecules change and the hydrogen bond shortens. 70,76 Lengths were calculated from previously published <sup>1</sup>H NMR chemical shifts of the hydrogen bonded protons using the empirical correlation between hydrogen bond O·O distance and  ${}^{1}H$  chemical shift  ${}^{98}$  (14.65 and 17.47 ppm for I and II, respectively  ${}^{129}$ ).  $pK_a$  values for the molecules shown: 2-choro-4-nitrophenol ( $pK_a = 5.4$ ), trifluoroacetate ( $pK_a = 0.2$ ), and trimethyl acetate ( $pK_a = 5.0$ ).  ${}^{130}$  (C) Variations in hydrogen bond O·O distances (n = 42) from X-ray crystal structures (n = 36) of 3,5-dinitrosalicylate. A histogram of the distances fits a normal distribution with an average distance of 2.462 Å and a standard deviation of 0.037 Å (Table S2).

structures, which are typically  $\leq$ 0.01 Å (Figure 1C, Table S2).  $^{52,55,81-83}$ 

Thus, additional factors must also contribute, to some extent, to hydrogen bond lengths. Inspection of the 3,5-dinitrosalicylate structures in Figure 1C reveal hydrogen bond networks with diverse hydrogen bonding patterns in different crystals and for different molecules within the crystal lattice (Table S2, Figure S4). Prior data, from us and others, has suggested that coupling between hydrogen bonds within networks may be one factor resulting in the observed differences in hydrogen bond length and we further investigate this effect herein. 70,84–89

Herein, we broadly demonstrate hydrogen bond coupling and quantitate its extent within hydrogen bond networks in three proteins: ketosteroid isomerase (KSI) from two sources, *Pseudomonas putida* (pKSI) and *Comamonas testosteroni* (tKSI), and photoactive yellow protein (PYP). 84,85 These

proteins have active site hydrogen bond networks (Figure 2) that can be readily manipulated to assess the effect of proximal

**Figure 2.** Hydrogen bond networks in the active sites of ketosteroid isomerase (KSI) and photoactive yellow protein (PYP). (A,B) pKSI (A) and tKSI (B) bound to a substituted phenolate transition state analog, and PYP (C) with covalently bound *p*-coumarate chromophore. Previous measurements in pKSI and tKSI, have shown that residue Asp103 in pKSI, and Asp99 in tKSI, have  $pK_a$  values that are >9, indicating that this residue is protonated at the neutral pH used herein. We were unable to obtain absorbance spectra of the F-Tyr variants bound to the phenolates used herein (DNP and TFMNP); however, absorbance spectra of F-Tyr variants with bound naphthol ligands indicate that these ligands are ionized, providing strong evidence that lower  $pK_a$  ligands such as DNP and TFMNP are also bound as anions (Text S2, Figure S2). He PYP protonation state is supported by a prior neutron diffraction study.

and distal perturbations, with the protein scaffold enforcing a conserved placement of groups. As a result, large conformational rearrangements that could alter the network connections are less problematic than in many small molecule systems, a supposition supported by high-resolution X-ray structural analysis. <sup>84,85</sup>, Vide infra <sup>1</sup>H NMR chemical shifts of highly downfield-shifted hydrogen bonded protons and highresolution X-ray crystallographic data of a series of enzyme variants with natural and unnatural amino acid substitutions have allowed us to determine coupling of hydrogen bond lengths between groups that donate hydrogen bonds to a common oxyanion acceptor. We have demonstrated that coupling is transmitted through two, three, and four hydrogen bonds in the network, with diminishing effects from more remote modifications. Remarkably, over the 19 perturbations made here and previously in three protein backgrounds, there is a single correlation for oxyanion hole hydrogen bond coupling. This agreement leads to a predictive, quantitative

model for these couplings and suggests a common underlying physical origin for this effect. Finally, hydrogen bond coupling was investigated in the oxyanion holes of pKSI and tKSI using molecular mechanics (MM) and quantum mechanics/molecular mechanics (QM/MM). Both methods described changes in the oxyanion hole hydrogen bond lengths due to perturbations to the proximal aspartic acid; however, MM methods did not reproduce length effects from perturbations of the distal hydrogen bond donors, presumably due to the lack of polarization in the rigid-charge MM force fields. High-precision mapping of hydrogen bond coupling is foundational for understanding protein dynamics and energetics, and may aid in evaluating computational models for protein conformational fluctuations and function.

# RESULTS AND DISCUSSION

The three proteins probed herein, ketosteroid isomerase (KSI) from two species (pKSI and pKSI), and photoactive yellow protein (PYP), each have a hydrogen bond network that includes a bound oxyanion ligand (Figure 2). For KSI, phenolates have been shown to act as transition state analogs, 90, vide infra and for PYP, p-coumarate is a covalently bound oxyanion that functions in the PYP photocycle. 91,5 Below, we first focus on coupling of the oxyanion hole hydrogen bonds, i.e., the two hydrogen bonds donated to active site-bound oxyanionic ligands. Oxyanion hole perturbations were made via unnatural amino acid incorporation for Tyr16 of pKSI and via site-directed mutagenesis for the aspartic acid or glutamic acid hydrogen bond donor, with mutation to asparagine or glutamine, respectively. As in previous studies, the Asp40Asn mutation in pKSI, and the corresponding Asp38Asn mutation in tKSI, were used to mimic the protonated general base in the enzyme intermediate complex and to increase phenolate affinities relative to Asp40 KSI. 50,93,94 Herein, all references to "WT KSI" contain this mutation and refer to proteins with the wild-type oxyanion hole configuration. Hydrogen bond length changes were determined using <sup>1</sup>H NMR spectroscopy and high-resolution X-ray crystallography, and the same coupling effects were observed by both techniques. After describing coupling between the oxyanion hole donors, we assess the effects on these hydrogen bonds from the more remote, networked hydrogen bond donors in each system. This coupling relationship was determined with two or three different bound ligands to further assess the accuracy of our results and the generality of this behavior. Remarkably, when we combine the structural information from all these measurements we observe a single linear relationship for the coupling of the oxyanion hole donors, regardless of the type of perturbation or protein identity. Finally, comparison of the experimental coupling to the relationships predicted by MM and QM/MM simulations provides insights into the origin of this effect. The hydrogen bond distance measurements and relationships determined experimentally, herein and previously, are summarized in Table 1 for ease of reference (Table 3 lists the values obtained computationally).

Structural Coupling of Hydrogen Bond Donors to a Common Acceptor. Previous results with tKSI and PYP revealed coupling between the oxyanion hole hydrogen bond lengths. Specifically, deuterium substitution is known to lengthen hydrogen bonds, and substitution of one of the two oxyanion hole hydrogen atoms by deuterium (via mixed H<sub>2</sub>O:D<sub>2</sub>O solutions) lengthened the other hydrogen bond

Table 1. Changes in Hydrogen Bond Lengths Determined by <sup>1</sup>H NMR and X-ray Crystallography Determined Herein and Previously

					1° H-Bond			2° H-Bond	
Protein	Perturbation	Ligand <sup>a</sup>	Method	Donor	$\Delta^{1 ext{H}}\delta$ (ppm)	ΔLength (Å)	Donor	$\Delta^{1H}\delta$ (ppm)	ΔLength (Å)
pKSI	Y32F	DNP	NMR	Y16	-0.61	0.024	D103	0.07	-0.003
	Y32F/Y57F		NMR	Y16	-3.19	0.151	D103	0.81	-0.030
	Y32F/Y57F		X-ray	Y16		0.10	D103		-0.04
	2-F-Y16 <sup>d</sup>		NMR	Y16	0.77	-0.029	D103	-0.13	0.005
	2,6-F <sub>2</sub> -Y16 <sup>d</sup>		NMR	Y16	1.55	-0.055	D103	-0.51	0.021
	D103N		X-ray	D103		$0.30 \ (0.17^b)$	Y16		-0.07
	Y32F	TFMNP	NMR	Y16	-0.69	0.023	D103	0.17	-0.006
	Y32F/Y57F		NMR	Y16	-3.65	0.156	D103	1.09	-0.035
	2-F-Y16 <sup>d</sup>		NMR	Y16	0.88	-0.029	D103	-0.21	0.007
	2,6-F <sub>2</sub> -Y16 <sup>d</sup>		NMR	Y16	1.84	-0.056	D103	-0.70	0.026
tKSI	F30Y	DNP	NMR	Y14	0.68	-0.025	D99	-0.30	0.012
	Y55F		NMR	Y14	-2.25	0.105	D99	0.62	-0.023
	D99N		NMR	D99	Ċ	Ċ	Y14	1.22	-0.045
	F30Y	TFMNP	NMR	Y14	0.60	-0.020	D99	-0.37	0.013
	Y55F		NMR	Y14	-2.56	0.111	D99	0.34	-0.013
	D99N		NMR	D99	c	c	Y14	1.51	-0.048
	Y55F	FTFMP	NMR	Y14	-3.23	0.111	D99	1.14	-0.031
PYP	T50 V	DNP	NMR	Y42	-0.96	0.051	E46	0.53	-0.025
	T50 V	TFMNP	NMR	Y42	-1.14	0.056	E46	0.30	-0.013
	T50 V <sup>85</sup>	p-CA	NMR	Y42	-1.3	0.059	E46	0.60	-0.019
	E46Q <sup>85</sup>		NMR	E46	d	d	Y42	1.50	-0.055
	E46Q <sup>111,112</sup>		X-ray	E46		$0.30 \ (0.17^{b})$	Y42		-0.05

 $^a$ 3,4-Dinitrophenolate (DNP; p $K_a$  = 5.4 $^{130}$ ), 3-(trifluoromethyl)-4-nitrophenolate (TFMNP; p $K_a$  = 6.3 $^{130}$ ), 3-fluoro-5-(trifluoromethyl)phenolate (FTFMP; p $K_a$  = 8.2 $^{130}$ ), p-coumaric acid (p-CA; p $K_a$  = 9.1 $^{85}$ )  $^b$ Distance corrected by 0.13 Å for comparison of N·O to O·O hydrogen bond distances (Text S3).  $^c$ The resonance corresponding to the Asp99-phenolate hydrogen bond is not seen in the downfield portion of this spectrum (Figure 4).  $^d$ The resonance corresponding to the Gln46-p-CA hydrogen bonded is not seen in the downfield portion of this spectrum (Figure S11).

(Figure 3A). <sup>84,85</sup> To further and systematically test coupling with minimal perturbation we turned to a set of unnatural amino acid substitutions for Tyr16, fluoro-substituted tyrosines (Figure 3B), which were previously shown to not have significant effects on function. <sup>95</sup>

F-Tyr16 Substitutions Shorten Tyr16-Oxyanion Hydrogen Bond and Lengthen the Asp103-Oxyanion Hydrogen Bond in pKSI. We prepared semisynthetic pKSI variants with tyrosine, 2-fluoro-tyrosine, and 2,6-difluoro-tyrosine at position 16 and used <sup>1</sup>H NMR to obtain information about hydrogen bond lengths. An empirical correlation function between <sup>1</sup>H chemical shifts and hydrogen bond lengths was previously established from direct comparisons of NMR and X-ray diffraction data on a large set of small-molecule crystals <sup>96–99</sup> and has been used extensively in hydrogen bond structure—function studies (e.g., refs 100–106). Upon closer approach of the hydrogen-bond acceptor (i.e., a shorter hydrogen bond), the O–H covalent bond distance lengthens, thereby deshielding the hydrogen-bonded proton to give a more downfield <sup>1</sup>H NMR chemical shift (Text S1). <sup>97–99,107</sup>

Previously, two short hydrogen bonds with highly deshielded protons were assigned to Tyr16 and Asp103 of the KSI oxyanion hole. With bound 3,4-dinitrophenolate (DNP), the two peaks are indistinguishable from one another, as expected based on extrapolation of chemical shifts previously observed for a series of bound substituted phenolates of varying  $pK_a$ : the chemical shifts that are distinct for higher- $pK_a$  phenolates converge for the low  $pK_a$  phenolates used herein ( $pK_a$  5.4 and 6.3) (Figure S5). Low  $pK_a$  phenolate ligands were used to avoid complications from potential internal proton transfers that can give bound phenols rather

than phenolates (Text S2).<sup>108</sup> With the fluoro-substituted tyrosines (Figure 3B), the expected two peaks are observed, with a downfield <sup>1</sup>H chemical shift migration that increases with larger p $K_a$  perturbations (Tyr  $\rightarrow$  F-Tyr  $\rightarrow$  F<sub>2</sub>-Tyr; Figure 3C, red) and an opposite, but smaller upfield migration of the second peak (Figure 3C, blue). The downfield peak migration matches the direction and scale for the  $pK_a$  variation at position 16, based on prior data for changes in hydrogen bond length with  $pK_a$  in this and other systems (Figures S4–S6). The second peak, which shifts upfield, is perturbed less and apparently represents a compensating lengthening of the Asp103 hydrogen bond in response to shortening of the F-Tyr16 hydrogen bond, as previously observed upon deuterium substitution. 84,85 We observed very similar effects with a second bound phenolate, providing independent support for these observations (3-(trifluoromethyl)-4-nitrophenolate, TFMNP, Figure 3D).

We used the literature relationship between <sup>1</sup>H chemical shift and hydrogen bond length (Text S1)<sup>97</sup> to convert the observed NMR results into hydrogen bond lengths (Table 1), and we plotted the change in hydrogen bond length for the F-Tyr16·oxyanion hydrogen bond versus the Asp103·oxyanion hydrogen bond (Figure 3E). The results are consistent with a linear correlation with a slope of approximately -0.4. This slope provides an initial estimate for the fold-change in Asp103·oxyanion hydrogen bond length observed upon a change in Tyr16·oxyanion hydrogen bond length. To extend this relationship to larger perturbations and to further test this correlation, we turned to the converse experiment, using site-directed mutagenesis to alter the KSI oxyanion hole aspartic

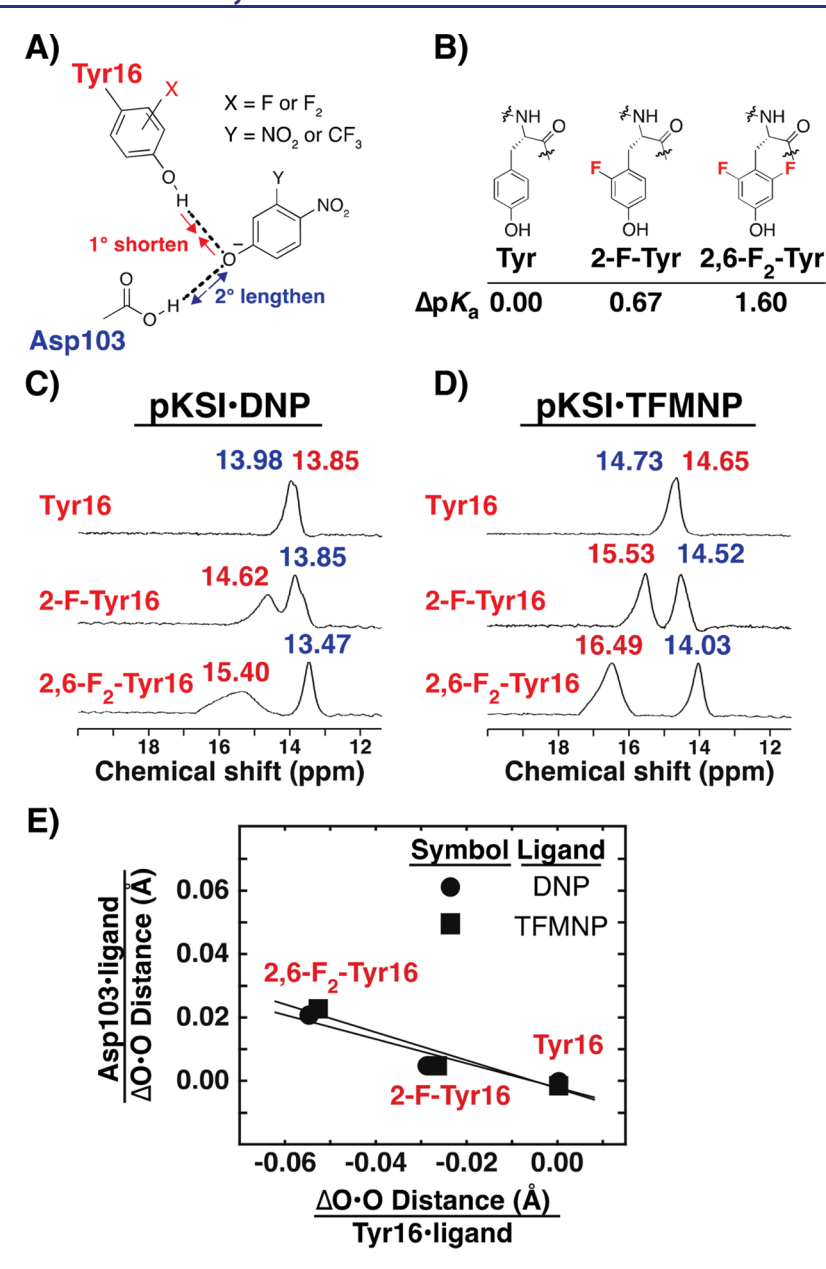


Figure 3. Changes in oxyanion hole hydrogen bond lengths upon F-Tyr substitution in pKSI determined from changes in <sup>1</sup>H NMR chemical shifts of the hydrogen-bonded protons. (A) Upon substitution of Tyr16 for 2-F-Tyr16 or 2,6-F<sub>2</sub>-Tyr16, the (F)-Tyr16-ligand hydrogen bond shortens and consequently the Asp103-ligand hydrogen bond lengthens. (B) (F)-Tyr residues used in semisynthetic variants and the change in  $pK_a$  for the corresponding phenols, relative to unsubstituted phenol, in water. (C,D) H NMR spectra of pKSI F-Tyr variants bound to DNP (C) and TFMNP (D). (E) Changes in Tyr16-phenolate versus Asp103-phenolate hydrogen bond lengths give slopes of -0.38 and -0.46 with bound DNP and TFMNP, respectively.

acid in both KSIs and the corresponding glutamic acid in PYP (Figure 2).

Lengthening the Asp-Oxyanion Hydrogen Bond Results in Shortening of the Tyr-Oxyanion Hydrogen Bond. To alter the Asp103·oxyanion hole hydrogen bond in pKSI we mutated Asp103 to Asn. The resulting mutant did not exhibit resolvable downfield <sup>1</sup>H chemical shifts with DNP or TMFNP bound, presumably due to rapid exchange between states or with solvent; this behavior and differential line broadening has been observed for several KSI/ligand combinations. (e.g. 84,90) As tKSI generally gives narrower NMR peaks, we made the analogous mutation in tKSI to interrogate hydrogen bond length changes by NMR, and we turned to high-resolution X-ray crystallography to analyze the hydrogen bonds in pKSI. To ensure that

we could accurately detect changes in hydrogen bond length by both methods, we characterized WT and mutant pKSI complexes (pKSI WT·DNP and pKSI Tyr32Phe/Tyr57Phe· DNP) by both <sup>1</sup>H NMR and X-ray crystallography (see below).

For WT tKSI with bound DNP, we see two nearby downfield <sup>1</sup>H resonances, at 14.07 and 13.94 ppm, previously assigned to the Tyr14-oxyanion and Asp99-oxyanion hydrogen-bonded protons (Figure 4A). 109 Upon mutation of the oxyanion hole aspartic acid to asparagine (Asp99Asn), a higher pK, hydrogen bond donor, one peak shifts downfield, representing hydrogen bond shortening, presumably of the Tyr14·DNP hydrogen bond. The other peak is no longer visible, presumably due to the lengthening of the Asp/Asn99·

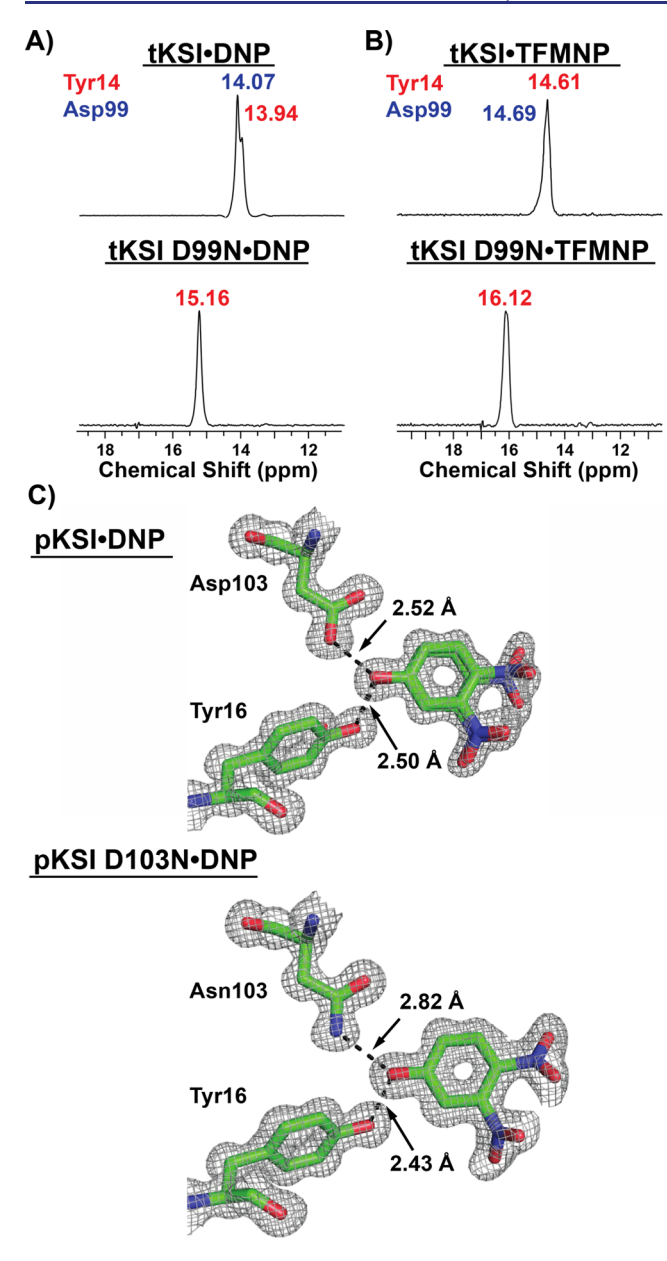


Figure 4. Coupling between KSI oxyanion hole hydrogen bonds upon mutation of Asp99 and Asp103 to asparagine in tKSI and pKSI, respectively. (A,B)  $^1\mathrm{H}$  NMR spectra of WT tKSI and tKSI Asp99Asn bound to (A) DNP or (B) TFMNP. NMR spectra for tKSI-DNP variants in panel A were also published in ref 84. (C) Hydrogen bond lengths from X-ray crystal structures of WT pKSI and pKSI Asp103Asn with bound DNP. Structures are contoured at  $1\sigma$  using PyMOL.

DNP hydrogen bond to an upfield region where there is interference from the multitude of protein <sup>1</sup>H peaks (Figure S8). As above, the same behavior was observed with an alternative bound phenolate (TFMNP, Figure 4B). These observations suggest that the oxyanion hole tyrosine hydrogen bond behaves analogously to what we observed above, i.e., upon lengthening (or shortening) of one hydrogen bond by perturbing that donor, the other hydrogen bond length responds oppositely. Nevertheless, we could not obtain a quantitative relationship between the two hydrogen bonds in this instance because we could not determine the Asn99-oxyanion hydrogen bond length.

To assess lengths changes for both hydrogen bonds upon substitution of Asp for Asn, we obtained high-resolution X-ray structures for WT and the Asp103Asn mutant of pKSI with bound DNP (1.05 and 1.10 Å, respectively; Table S3; Figure 4C). At these resolutions, the measured changes in hydrogen bond length are significantly beyond the error estimates calculated from the coordinate errors of the hydrogen bonded atoms (Table S4,5 and see Methods), and we observed the same trends as described above. Structures of pKSI-DNP and pKSI D103N·DNP overlay with a root-mean-square deviation of 0.23 Å (see Methods) for backbone atoms, and there is no indication of significant rearrangements in the active site or surrounding structure (Figure S9). For pKSI·DNP, the Asp103·DNP hydrogen bond distance is 2.52 Å, whereas in the pKSI D103N·DNP structure the average Asn103·DNP hydrogen bond distance is 2.82 Å (Figure 4C), and the 0.30 Å difference in hydrogen bond length is well outside the distance error estimate of 0.03 Å (Table S5). N·O hydrogen bonds, such as the Asn103·DNP hydrogen bond, are on average 0.13 Å longer than O·O hydrogen bonds, due to the larger van der Waals radii of nitrogen compared to oxygen (Text S3).51,110 Accounting for the observed N·O hydrogen bond distance by subtracting 0.13 Å to allow direct comparison with the Asp103 O·O hydrogen bond gives an apparent change in the Asp/ Asn103 hydrogen bond length of 0.17 Å, although omitting this distance correction does not alter interpretation of these results (Figure S10). Accompanying the lengthening of the Asp/Asn103 hydrogen bond is shortening of the Tyr16·DNP hydrogen bond, from 2.50 to 2.43 Å (Figure 4C). Though small, this shortening of 0.07 Å is beyond the estimated error of 0.03 Å (Table S5) and is consistent with the analogous shortening of the tKSI Tyr14·DNP hydrogen bond by 0.045 Å determined by <sup>1</sup>H NMR (Figure 3A). These results again suggest coupling between the two oxyanion hole hydrogen bonds (Table 1).

To further investigate the commonality of this coupling, we compared previous high-resolution PYP structures for WT and Glu46Gln PYP obtained at 1.25 and 1.20 Å resolution, respectively. Mutation of Glu46 to Gln46 results in a lengthening of the Glu/Gln46·*p*-coumarate hydrogen bond by 0.30 Å, from 2.56 to 2.86 Å (Figure S11; Table 1). This lengthening is accompanied by a 0.05 Å shortening of the Tyr42·*p*-coumarate hydrogen bond, a result also supported by previously published <sup>1</sup>H NMR spectra, with hydrogen bond shortening calculated to be 0.055 Å (Figure S11; Table 1) and very similar to the KSI results.

Remote Hydrogen Bond Perturbations. The experiments above establish strong coupling of hydrogen bond lengths between two hydrogen bonds with a common acceptor. But to what extent are hydrogen bonds structurally coupled to more remote hydrogen bonds throughout a network? In pKSI, Tyr16 accepts a hydrogen bond from Tyr57, which in turn accepts a hydrogen bond from Tyr32 (Figure 2A). To assess more remote effects, we mutated Tyr57 and Tyr32 to phenylalanine and obtained <sup>1</sup>H NMR spectra with bound DNP and TFMNP. With both phenolate ligands, far downfield <sup>1</sup>H chemical shifts were observed as expected for the oxyanion hole hydrogen bonds. We present the TFMNP data first, as the <sup>1</sup>H peaks were better resolved (Figure 5A,B). As Tyr57 interacts directly with Tyr16, the largest change in chemical shift is expected to be from a change in the Tyr16· TFMNP hydrogen bond length. A smaller change, in the opposite direction, would then be predicted for the Asp103.

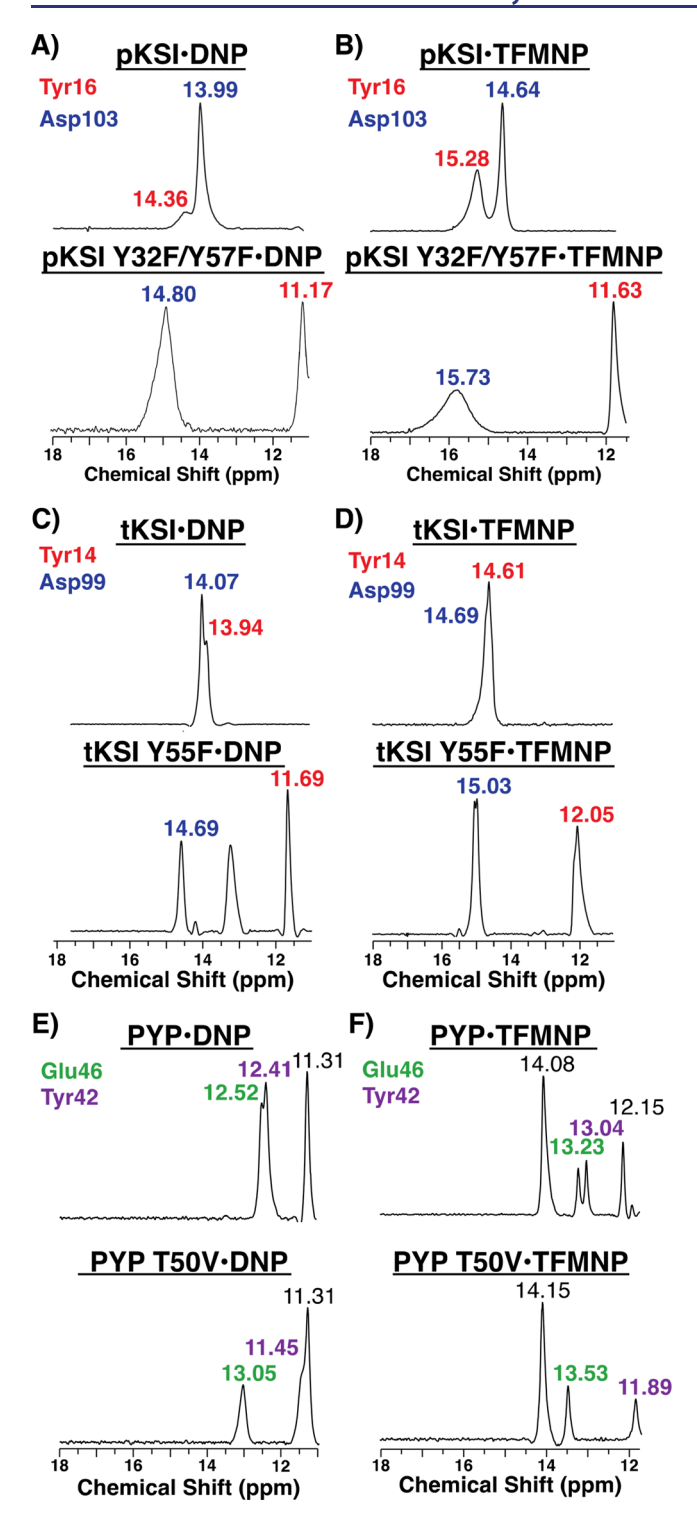


Figure 5. Adjacent hydrogen bond donors, Tyr57 in pKSI, Tyr55 in tKSI, and Thr50 in PYP, influence oxyanion hole hydrogen bond lengths. (A,B) ¹H NMR spectra of pKSI WT and Tyr32Phe/Tyr57Phe bound to DNP (A) or TFMNP (B). (C,D) ¹H NMR spectra of tKSI WT and Tyr55Phe bound to DNP (C) or TFMNP (D). A third peak is observed in the spectra of tKSI Y55F·DNP at 13.2 ppm. This peak has been observed in previously published NMR spectra of tKSI<sup>84</sup> and has a chemical shift that is invariant with different bound ligands<sup>84</sup> and is not observed in the other tKSI spectra herein presumably due to rapid exchange. (E,F) ¹H NMR spectra of PYP WT and Thr50Val variants bound to DNP (E) or TFMNP (F). Two additional peaks are observed in the PYP spectra with bound TFMNP: one downfield peak at ~14.1 ppm, which is

Figure 5. continued

visible in both WT and Thr50Val spectra, and one at 12.15 ppm, which disappears upon Thr50Val mutation. The identity of these peaks is unknown, and are not observed in other  $^1\mathrm{H}$  NMR spectra of PYP.  $^{85}$  The assignment of the oxyanion hole hydrogen bond peaks to the peaks at 13.04 and 13.23 ppm with bound DNP and TFMNP, respectively is supported by the linear correlation between chemical shift and phenolate  $pK_a$  for previously published spectra of PYP, which predicts chemical shifts of 13.09 and 13.19 ppm for TFMNP ( $pK_a$  6.3) (Figure S6).

TFMNP hydrogen bond. In <sup>1</sup>H NMR spectra of pKSI Tyr32Phe/Tyr57Phe bound to TFMNP, one peak moves upfield from 15.28 to 11.63 ppm, while the other moves downfield from 14.63 to 15.73 ppm (Figure 5B, Table 1).1 The larger upfield change is presumably due to the lengthening of the Tyr16·TFMNP hydrogen bond. This lengthening is supported by a 1.06 Å X-ray structure of pKSI Tyr32Phe/ Tyr57Phe bound to DNP, which shows a 0.10 Å longer Tyr16· DNP hydrogen bond in the Tyr57Phe/Tyr32Phe background compared to WT (see Figure 8 below). The smaller downfield change in chemical shift is presumably due to the coupled response of the Asp103·TFMNP hydrogen bond. The same behavior is seen in <sup>1</sup>H NMR spectra for pKSI with bound DNP and in tKSI with bound DNP and TFMNP, (Figure 5A-D), and also with a third ligand, 3-fluoro-5-(trifuoromethyl)phenolate (FTFMP,  $pK_a$  8.2) (Figure S12).

The oxyanion hole tyrosine of PYP accepts a hydrogen bond from Thr50 (Figure 2C), and the effects from mutating this residue are analogous to those observed for the hydrogen bond network mutations in tKSI and pKSI. Previously published <sup>1</sup>H NMR spectra for PYP WT and Thr50Val with the covalently bound p-coumarate (p-CA) ligand show that upon mutation of Thr50 to valine, one peak shifts upfield by 1.3 ppm, while the other shifts downfield by 0.6 ppm (Figure S11).85 These peaks were previously assigned to Tyr42 and Glu46, respectively, and correspond to a 0.058 Å lengthening of the Tyr42·p-CA hydrogen bond and a 0.019 Å shortening of the Glu46·p-CA hydrogen bond (Table 1).85 Although the scale of oxyanion hole hydrogen bond coupling is the same in PYP as in KSI, the magnitude of the length changes from mutating Thr50 in PYP are smaller than the effects of mutating Tyr55 in tKSI or Tyr32/Tyr57 in pKSI. This smaller effect may reflect the different properties of the Thr hydrogen bond donor compared to Tyr (p $K_a$  16 vs 10, respectively), which is a less effective donor and will have a smaller effect on the neighboring hydrogen bonds. As PYP is also known to bind phenolates, we collected <sup>1</sup>H NMR spectra of PYP WT and PYP Thr50Val with bound DNP and TFMNP.85 In both cases, the coupling between the oxyanion hole hydrogen bonds matches that seen with p-CA (Figure 5E,F; Table 1).

The hydrogen bond network in pKSI has an additional tyrosine residue, Tyr32, allowing us to determine the extent of coupling from a hydrogen bond donor that has an intervening hydrogen bond separating it from the oxyanion hole. A simple expectation is that the Tyr32Phe mutation would result in length changes in the same direction as the Tyr32Phe/Tyr57Phe mutation above, but smaller in magnitude. Mutation of Tyr32 to phenylalanine in pKSI bound to DNP resulted in changes in the oxyanion hole chemical shifts, with one peak moving upfield by 0.61 ppm and the other downfield by 0.07 ppm, corresponding to a lengthening of the Tyr16·DNP

hydrogen bond by 0.024 Å and a shortening of the Asp103· hydrogen bond by 0.003 Å (Figure 6A, Table 1). As expected,

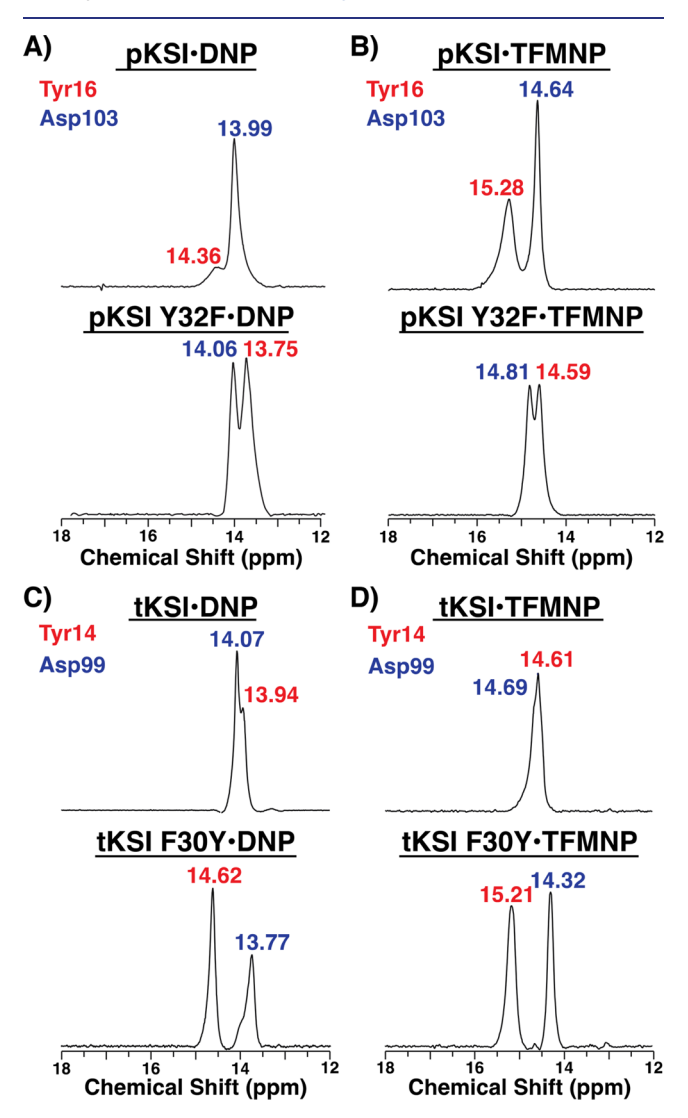


Figure 6. Remote hydrogen bond donors are coupled to oxyanion hole hydrogen bonds. (A,B) <sup>1</sup>H NMR spectra of pKSI WT and Tyr32Phe variants bound to DNP (A) or TFMNP (B). (C,D) <sup>1</sup>H NMR spectra of tKSI WT and Phe30Tyr variants bound to DNP (C) or TFMNP (D).

the scale of these couplings matches the previous results above, but with magnitudes 6-10-fold smaller than the effects from Tyr32Phe/Tyr57Phe mutation. The same behavior is seen with bound TFMNP (Figure 6B).

tKSI lacks a tyrosine residue homologous to Tyr32 of pKSI, having instead a phenylalanine at that position (Figure 2B). In the simplest case, the Phe30Tyr mutation in tKSI would have an opposite effect from the Tyr32Phe mutation in pKSI, i.e., shortening the Tyr14 hydrogen bond and lengthening the Asp99 hydrogen bond, and indeed this was observed (Table 1). Upon introducing the Phe30Tyr mutation into tKSI, the <sup>1</sup>H NMR spectra with bound DNP changes such that there is a shortening of the Tyr14·DNP hydrogen bond and a lengthening of the Asp99·DNP hydrogen bond. Analogous coupling was seen with bound TFMNP (Figure 6D; Table 1).

Our results suggest that coupling of the oxyanion hole hydrogen bond to remote tyrosine residues is due to

polarization from these adjacent hydrogen bond donors on Tyr16 (see "A Uniform Scale for Hydrogen Bond Length Coupling in KSI and PYP" below). To compare effects on hydrogen bond length from the distal network participants to the effects from direct changes of the oxyanion hole hydrogen bond donors, we created a common scale for these changes. We used the known aqueous  $pK_a$  values, and utilized the hydrogen bond length effects, for the pKSI F-Tyr substitutions, above, to relate the Tyr16·DNP hydrogen bond length to changes in Tyr16 pKa, which can be thought of in terms of changes in the electronic properties of this residue (Figure This relationship gave a slope of 0.034  $Å/pK_3$ ,

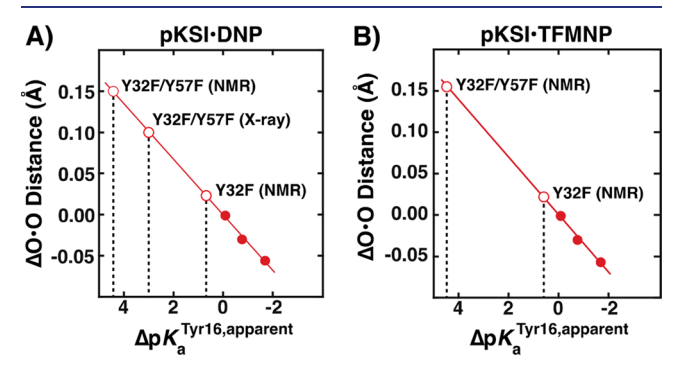


Figure 7. Estimation of changes in the "apparent  $pK_a$ " of Tyr16 in Tyr32Phe/Tyr57Phe and Tyr32Phe mutants of pKSI. Changes in Tyr16·oxyanion (solid circles) hydrogen bond lengths are plotted versus the  $pK_a$  of the residue present at position 16, relative to the parent Tyr (from Figure 3) bound to either DNP (A) or TFMNP (B). Assuming a linear relationship, changes in oxyanion hole hydrogen bond lengths from Tyr32Phe/Tyr57Phe and Tyr32Phe mutations are placed on the line of best fit (open circles) and apparent p $K_a$  values for Tyr16 in each mutant are read from the X-axis (dotted lines). Values are reported in Table S9.

similar to the slope observed for changes in hydrogen bond length with  $\Delta p K_a$  between donor and acceptor atoms in small molecule crystals (Figure 1A).<sup>70</sup> Using this relationship, the 0.151 Å lengthening of the Tyr16·DNP hydrogen bond from the Tyr32Phe/Tyr57Phe mutation corresponds to an increase in the apparent  $pK_a$  of Tyr16 by 4.5  $pK_a$  units (Figure 7A; Table S8). The Tyr32Phe mutation alone corresponds to a smaller increase in the apparent p $K_a$  of Tyr16 of 0.7 p $K_a$  units (Figure 7A; Table S8). Similar changes were found for pKSI bound to TFMNP and from X-ray structures of pKSI-DNP and pKSI Tyr32Phe/Tyr57Phe·DNP (Figure 7A,B; Table S8).

These mutational effects perturb the apparent  $pK_a$  of Tyr16 in the expected direction. The "desolvation" of Tyr16 by removal of the Tyr57 hydrogen bond (and replacement by Phe) is expected to decrease the polarity of the Tyr16 hydroxyl group and thus make it a weaker hydrogen bond donor, with a longer hydrogen bond, as is observed. We emphasize that the estimated apparent  $pK_3$  is a measure of the properties of the neutral Tyr16, and one does not expect its measured  $pK_a$  to correspond to this value, as the measured  $pK_a$  reports on the change in the electronic properties of Tyr16, as well as changes to the tyrosinate anion, including possible active site rearrangements and changes in access to solvating water molecules, that are not relevant to the original hydrogen bonded state.  $^{115}$  The value of estimating an apparent p $K_{\rm a}$  of Tyr16 lies in the ability to compare values for different perturbations on a common scale.

Comparison of NMR- and X-ray-Derived Hydrogen Bond Distances. Though analyses of hydrogen bond length changes on the scales observed herein are common by <sup>1</sup>H NMR (e.g., refs 100–106), it is less common to draw conclusions about small length changes from X-ray data. Thus, even with our very high-resolution structures and estimated distance errors that are much smaller than the observed changes, we wanted additional empirical evidence. We therefore obtained a high-resolution X-ray structure for pKSI Tyr57Phe/Tyr32Phe with bound DNP (1.06 Å; Figure 8) and compared it to pKSI WT·DNP (1.10 Å) (Figure 4C), <sup>116</sup> as we had corresponding <sup>1</sup>H NMR data for these complexes.

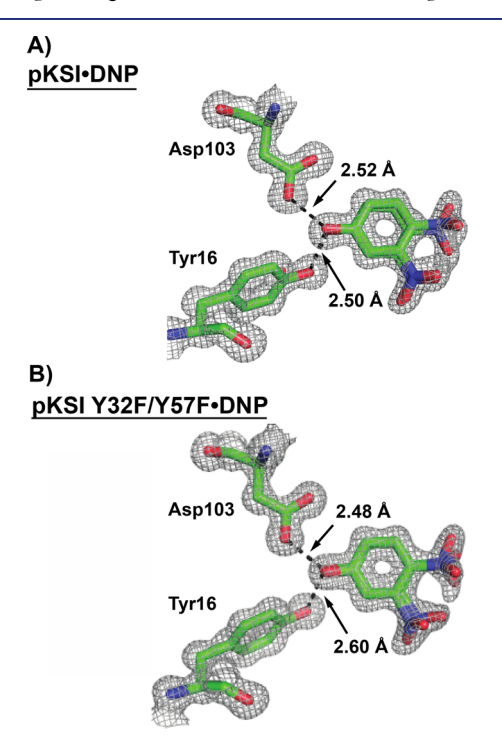
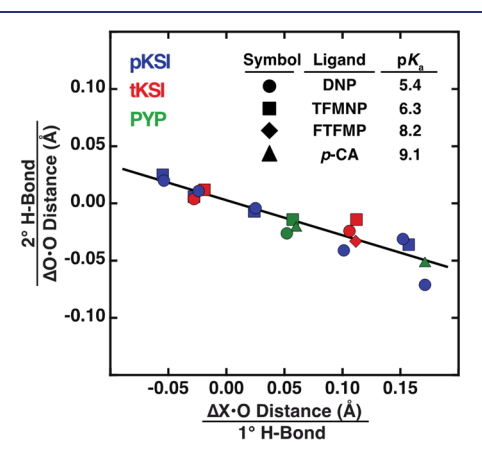


Figure 8. Comparison of oxyanion hole hydrogen bond lengths in X-ray crystal structures of pKSI·DNP and pKSI Tyr32Phe/Tyr57Phe-DNP. (A,B) Oxyanion hole hydrogen bond lengths from the 1.10 Å X-ray crystal structure of pKSI·DNP (A) (also shown in Figure 4C) are compared to the oxyanion hole hydrogen bond lengths from the 1.06 Å X-ray crystal structure of pKSI Tyr32Phe/Tyr57Phe (B). Structures are contoured at  $1\sigma$  using PyMOL.

The changes in hydrogen bond lengths determined by X-ray crystallography and <sup>1</sup>H NMR were in excellent agreement (Figure 8, Table 2), providing support for the accuracy of both methods and further support for the chemical shift assignments used above. Nevertheless, the absolute hydrogen bond lengths

determined by NMR were systematically longer than those determined by X-ray crystallography (Table 2), and an analogous discrepancy is seen in a broader correlation of hydrogen bond lengths vs  $\Delta p K_a$  for a wide variety of small molecule compounds.<sup>68</sup> This discrepancy may arise from an oversimplified functional form for conversion of <sup>1</sup>H chemical shifts into distances, from limited data in the standard curve, and/or from additional factors that alter the absolute chemical shifts but not their differences. These effects do not affect the conclusions herein.

Uniform Scale for Hydrogen Bond Length Coupling in KSI and PYP. In all of the tested cases thus far, 22 in total, 117 length coupling was observed between the oxyanion hole hydrogen bonds. To determine whether these reciprocal changes are quantitatively consistent, we plotted the change in the "primary" hydrogen bond length, corresponding to the hydrogen bond with the largest effect from unnatural amino acid incorporation or site-directed mutagenesis, versus the change in hydrogen bond length for the other ("secondary") oxyanion hole hydrogen bond (Figure 9). The data for all three



**Figure 9.** Uniform coupling between oxyanion hole hydrogen bonds. The "1° H-Bond" is the oxyanion hole hydrogen bond most directly affected by the perturbation (e.g., the Asp103-phenolate hydrogen bond for an Asp103Asn mutation in pKSI), and the "2° H-Bond" is the other oxyanion hole hydrogen bond (i.e., in this example, Tyr16-phenolate hydrogen bond). For the "1° H-Bond", X is either O or N. The slope of the line of best fit is  $-0.30 \pm 0.03$  ( $R^2 = 0.87$ ). Slopes and  $R^2$  values for fits to data for individual proteins give similar values (pKSI slope = -0.31,  $R^2 = 0.89$ ; tKSI slope = -0.26,  $R^2 = 0.90$ ; PYP slope = -0.27,  $R^2 = 0.89$ ). Data are summarized in Table 1. The hydrogen bond distances involving an N(H) hydrogen bond donor were corrected as described in Text S3.

proteins, pKSI, tKSI and PYP, follow a single correlation with a slope of  $-0.30 \pm 0.03$ ; i.e., in response to a change in primary

Table 2. Comparison of pKSI Hydrogen Bond Lengths and Length Changes Determined by <sup>1</sup>H NMR and X-ray Crystallography<sup>a</sup>

		Hydrogen B	ond Length (Å)	
	Tyr16	5-DNP	Asp10	3·DNP
Variant	NMR	X-ray	NMR	X-ray
pKSI·DNP	$2.58 \pm 0.041$	$2.50 \pm 0.025$	$2.60 \pm 0.034$	$2.52 \pm 0.024$
pKSI Y32F/Y57F●DNP	$2.73 \pm 0.030$	$2.60 \pm 0.019$	$2.57 \pm 0.041$	$2.48 \pm 0.018$
$\Delta(O \bullet O \text{ Length}) \text{ (Å)}$	$0.15 \pm 0.05$	$0.10 \pm 0.03$	$-0.03 \pm 0.05$	$-0.04 \pm 0.03$

<sup>&</sup>quot;Errors for X-ray distances are estimated from coordinate errors of hydrogen bonding atoms (Table S5). Errors for NMR-derived distances are estimated from the empirical fit used to convert chemical shifts to distances (Text S1).

hydrogen bond length, the secondary hydrogen bond changes in the opposite direction by a factor of  $0.30 \pm 0.03$ . This common coupling scale between the three proteins occurs regardless of specific perturbation or the site of perturbation within the network. The uniformity of this scale suggests that the response to perturbations is the result of propagated polarization and induction effects through the network. The different position of groups within the hydrogen bond networks would be expected to yield differential effects on the two oxyanion hole hydrogen bonds if these effects were propagated through space instead of through bond. By this model, the Tyr57Phe mutation in pKSI alters the Tyr16phenolate hydrogen bond length, which in turn alters the Asp103-phenolate hydrogen bond. In support of minimal through-space effects, mutation of Arg52 to alanine in PYP, which is 4.53 Å from Thr50 and 6.36 Å from the anionic chromophore, but not linked by a hydrogen bond network (Table S7), had no effect on the oxyanion hole hydrogen bond lengths; despite its close proximity and charge. (Figure S13).

The same coupling scale applies to all three proteins, despite differences in the sequence and structure of their surrounding scaffolds. tKSI and pKSI are 34% identical and vary in many second and third shell residues (Figure S14). Given the observed drop-off in effects for perturbations of more remote hydrogen bond donors, we looked specifically at nearby residues with significant dipoles. pKSI has five methionine residues located close to the active site hydrogen bond network, whereas tKSI has just one nearby methionine (within 10 Å) (Table S8). Even though methionine has a significant dipole moment ( $\mu_{\text{Met}} = 1.6 \text{ D}$ ), <sup>118</sup> there are either no differences in coupling between pKSI and tKSI, or, seemingly much less likely, differential effects that are coincidentally compensated by other dissimilarities. PYP, which is unrelated to KSI and has very different residues surrounding the active site (Figure S14), still follows the same correlation, further suggesting that scaffold architecture and residues outside of hydrogen bond networks are not primary determinants of hydrogen bond lengths and coupling within networks. Additionally, the exclusion of water from the active sites of enzymes by the close packing of second shell residues may prevent the formation of additional hydrogen bonding interactions with water, which would be expected alter hydrogen bond lengths based on the coupling relationship observed herein, dependent on their partners and number.

We observed indistinguishable coupling with oxyanion ligands with  $pK_a$  values ranging from 5.4-9.1, but future studies will be required to determine if larger variations in oxyanion character affect coupling, as an increase in charge density and polarizability of the central acceptor atom (here an oxyanion) might be expected to lead to increases in coupling. Our data also suggested consistency when at least one N-H hydrogen bond donor was added to the network, provided that we corrected for the generally longer N·O hydrogen bonds (Figure S3). However, additional data with nitrogen and other heteroatom hydrogen bond donors and acceptors will be needed to further extend and test this predictive model, as well as test the origins of the observed effects. Additional experiments will also be needed to extend these observations to other hydrogen bond networks with different geometries and charge.

A corollary of the above single correlation is that the coupling of the oxyanion hole hydrogen bond lengths is commutative, i.e., the secondary hydrogen bond length effects

J

are the same whether the tyrosine or carboxylic acid oxyanion hole donor was perturbed. Given this, and the effect of more remote residues on the oxyanion hole, we expect that changes in oxyanion hole donors, and thus changes in lengths of the oxyanion hole hydrogen bonds, will also propagate to the more remote network hydrogen bonds (e.g., Tyr16·Tyr57 and Tyr57·Tyr32 hydrogen bonds in pKSI; Figure 2). Our X-ray structural models show an observed lengthening of the Tyr16·Tyr57 hydrogen bond by 0.02 Å (2.52 to 2.54 Å) from the Asp103Asn mutation in pKSI, but this is on the order of the estimated distance error (Table S5, Figure S15); we do not have a <sup>1</sup>H NMR signal for this hydrogen bond, which would allow a more precise determination. Thus, we can conclude that any such effect is small, as expected for a remote effect, but we cannot assign a value to it.

Quantum Mechanics/Molecular Mechanics (QM/MM) and Molecular Mechanics (MM) Simulations of Hydrogen Bond Coupling in KSI. The experimentally observed hydrogen bond coupling provided an opportunity to test the ability of computational methods to reproduce experiment and to contribute to the development of mechanistic models. We compared hydrogen bond coupling trends determined in experiment to MM and QM/MM simulations of pKSI and tKSI bound to the DNP ligand. To minimize bias, MM and QM/MM simulations of pKSI and tKSI were carried out distinct from experiments described above and results were not shared prior to the development and implementation of the calculations. We first describe the determination of the QM region for the QM/MM model, and then compare hydrogen bond coupling and absolute hydrogen bond distances in the MM and QM/MM models.

To determine the optimum QM region for the QM/MM simulations, we assessed the effect of QM region size on the oxyanion hole hydrogen bond lengths in a single pKSI·DNP structure with QM regions consisting of 31 to 966 atoms (Figure 10). A small QM region consisting of only the DNP ligand and the Tyr16 side chain (Figure 10; QM1; 31 atoms) resulted in a Tyr16·DNP hydrogen bond distance of ~2.62 and ~2.64 Å using ω-PBEh and B3LYP-D3 exchange correlation functionals, respectively. Both exchange correlation functionals resulted in longer Tyr16·DNP hydrogen bond distances when compared to the 2.50 Å observed in the X-ray crystal structure. When the QM region was increased to include the entire active site hydrogen bond network (Figure 10; QM3; 68 atoms) the computed Tyr16·DNP hydrogen bond length with  $\omega$ -PBEh and B3LYP-D3 shortened to similar lengths of ~2.60 and ~2.59 Å, respectively. A further increase in size to 966 atoms resulted in convergence difficulties when using B3LYP-D3 due to the delocalization errors in DFT treatments of exchange-correlation, but showed little additional change with  $\omega$ -PBEh, which is less sensitive to delocalization errors since it includes exact exchange at long-range. 119-122 Given the convergence of hydrogen bond lengths at QM3, the 68 atom QM region was chosen for the pKSI and tKSI simulations below.

To compare experimental and computational coupling values, analogous hydrogen bond network perturbations were made *in silico* and changes in hydrogen bond lengths were compared. Two sets of mutations were made: mutation of the oxyanion hole aspartic acid to asparagine (Asp103Asn and Asp99Asn in pKSI and tKSI, respectively) and mutation of the remote tyrosine hydrogen bond donors to phenylalanine

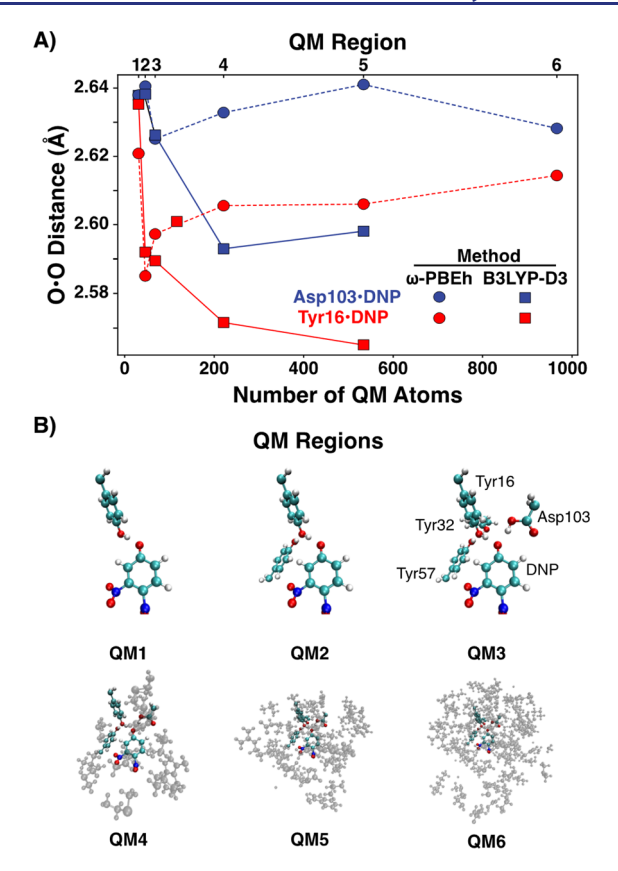


Figure 10. Relationship between oxyanion hole hydrogen bond lengths and QM region size in WT pKSI bound to DNP with ω-PBEh (circle) and B3LYP-D3 (square) and the 6-31G\*\* basis set. (A) Lengths of the oxyanion hole hydrogen bonds, Asp103·DNP (blue) and Tyr16·DNP (square), in the selected QM regions shown in panel B. (B) QM regions for lengths shown in panel A. QM3, which includes the side chains of the pKSI hydrogen bond network, Tyr16, Tyr57, Tyr32, Asp103 and DNP (68 atoms), was chosen as the QM region size.

(Tyr32Phe/Tyr57Phe and Tyr55Phe in pKSI and tKSI, respectively).

In the high-resolution X-ray crystal structures of WT pKSI-DNP and pKSI Asp103Asn·DNP, mutation of Asp103Asn lengthened the Asp/Asn103·DNP hydrogen bond from 2.52 to 2.82 Å and shortened the Tyr16·DNP hydrogen bond from

2.50 to 2.43 Å (Figure 4C). This coupling is reproduced in both MM and QM/MM simulations, although the magnitudes of these length changes are smaller than experiment in both MM and QM/MM simulations by 20-60% (Figure 11A; Table 3). The change in length of the Asp/Asn103·DNP hydrogen bond was  $0.09 \pm 0.04$  and  $0.11 \pm 0.04$  Å in MM and QM/MM, respectively, compared to  $0.17 \pm 0.03$  Å from X-ray (these values are corrected for longer N·O hydrogen bonds (see text S3); uncorrected values are 0.22, 0.24, and 0.30 Å for MM, QM/MM and X-ray, respectively). This difference is largely due to longer Asp103·DNP hydrogen bond lengths in MM and QM/MM than experiment (2.60  $\pm$  0.02 and 2.59  $\pm$ 0.03 Å, respectively, compared to 2.52  $\pm$  0.03 Å from X-ray, (Table 3)) and suggests that predicting the shortest hydrogen bonds may be difficult (see below). Analogous results were obtained in MM and QM/MM simulations of WT tKSI-DNP and Asp99Asn·DNP (Figure 11C; Table 3), providing evidence for the robustness of the approaches used.

Mutation of the remote hydrogen bond donors Tyr32 and Tyr57 to phenylalanine in pKSI·DNP results in lengthening of the Tyr16·DNP hydrogen bond and shortening of the Asp103·DNP hydrogen bond, as observed by both <sup>1</sup>H NMR and X-ray crystallography (Table 1). QM/MM showed an increase in Tyr16·DNP length of 0.11 ± 0.04 Å, closely matching the 0.10 and 0.15 Å increase seen by X-ray crystallography and NMR, respectively (Figure 11B Table 3). In contrast, there is no significant change in Tyr16·DNP hydrogen bond length from the Tyr32Phe/Tyr57Phe mutation in the MM simulations (0.04 ± 0.04 Å; Figure 11B; Table 3). This difference may arise from the ability of QM/MM to account for induction and polarizations effects from Tyr57 and Tyr32 that are not present in MM simulations. Analogous results were obtained for the tKSI Tyr55Phe mutant (Figure 11D).

To further evaluate these models, we compared absolute hydrogen bond lengths from the MM and QM/MM simulations to experiment. We anticipate that hydrogen bond lengths will be better defined in simulations of small molecules compared to the large protein system we used herein where multiple approximations must be made. Potential sources of error are described in the Supplementary Methods. In the case of the pKSI Asp103Asn variant bound to DNP, the Asn103-DNP hydrogen bond lengths determined by MM and QM/MM were  $2.82 \pm 0.02$  and  $2.83 \pm 0.03$  Å, respectively, closely matching the X-ray experimental value of  $2.82 \pm 0.02$  Å (Table

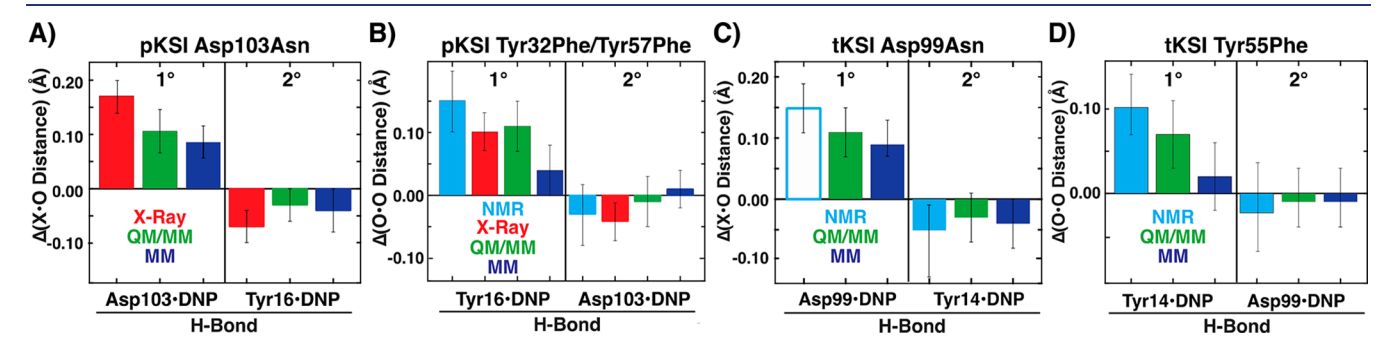


Figure 11. Comparison of hydrogen bond length coupling from experiment and from MM and QM/MM simulations of pKSI (A,B) and tKSI (C,D). (A–D) Changes in primary and secondary hydrogen bond lengths for pKSI Asp103Asn (A) and Tyr32Phe/Tyr57Phe (B) mutants and tKSI Asp99Asn (C) and Tyr55Phe (D) mutants determined by X-ray crystallography (red), NMR (cyan), QM/MM (green), and MM (blue). The primary change in Asp/Asn99·DNP length was not resolvable by <sup>1</sup>H NMR (Figure 4A), so this value was estimated based on the change in Tyr14-DNP hydrogen bond length and the coupling relationship in Figure 9 (open square in panel C). The hydrogen bond distances involving an N(H) hydrogen bond donor were corrected as described in Text S3.

Table 3. Hydrogen Bond Lengths and Length Couplings from MM and QM/MM Simulations<sup>a</sup>

			MM	ď	QM/MM	X	X-ray	Ń	NMR
Protein	Variant	Y16-DNP	D(N)103·DNP	Y16-DNP	D(N)103·DNP	Y16-DNP	D(N)103·DNP	Y16-DNP	D(N)103·DNP
pKSI	WT	$2.64 \pm 0.03$	$2.60 \pm 0.02$	$2.55 \pm 0.02$	$2.59 \pm 0.03$	$2.50 \pm 0.02$	$2.52 \pm 0.02$	$2.58 \pm 0.04$	$2.60 \pm 0.03$
	Y32F/Y57F	$2.68 \pm 0.03$	$2.61 \pm 0.02$	$2.66 \pm 0.04$	$2.58 \pm 0.03$	$2.60 \pm 0.02$	$2.48 \pm 0.02$	$2.73 \pm 0.03$	$2.57 \pm 0.04$
	D103N	$2.60 \pm 0.02$	$2.82 \pm 0.02$	$2.52 \pm 0.02$	$2.83 \pm 0.03$	$2.43 \pm 0.02$	$2.82 \pm 0.02$		
		Y14-DNP	D(N)99.DNP	Y14.DNP	D(N)99·DNP	Y14.DNP	D(N)99·DNP	Y14-DNP	D(N)99.DNP
tKSI	WT	$2.66 \pm 0.02$	$2.60 \pm 0.03$	$2.56 \pm 0.03$	$2.58 \pm 0.03$			$2.60 \pm 0.03$	$2.59 \pm 0.04$
	YSSF	$2.68 \pm 0.04$	$2.59 \pm 0.02$	$2.63 \pm 0.03$	$2.57 \pm 0.03$			$2.70 \pm 0.03$	$2.57 \pm 0.04$
	N66Q	$2.62 \pm 0.03$	$2.82 \pm 0.03$	$2.53 \pm 0.02$	$2.82 \pm 0.03$			$2.55 \pm 0.02$	
					$\Delta$ (Hydrogen Bond Length) $(A)^b$	$\operatorname{ingth}(A)^b$			
			MM	ď	QM/MM		X-ray		NMR
Protein	Variant	Y16-DNP	D(N)103·DNP	Y16-DNP	D(N)103·DNP	Y16-DNP	D(N)103·DNP	Y16.DNP	D(N)103·DNP
pKSI	Y32F/Y57F	$0.04 \pm 0.04$	$0.01 \pm 0.03$	$0.11 \pm 0.04$	$-0.01 \pm 0.04$	$0.10 \pm 0.03$	$-0.04 \pm 0.03$	$0.15 \pm 0.05$	$-0.03 \pm 0.05$
	D103N	$-0.04 \pm 0.04$	$0.22 (0.09^a) \pm 0.03$	$-0.03 \pm 0.03$	$0.24 (0.11^a) \pm 0.04$	$-0.07 \pm 0.03$	$0.30 (0.17^a) \pm 0.03$		
		Y14.DNP	D(N)99.DNP	Y14-DNP	D(N)99.DNP	Y14-DNP	D(N)99.	Y14-DNP	D(N)99.DNP
tKSI	YSSF	$0.02 \pm 0.04$	$-0.01 \pm 0.04$	$0.07 \pm 0.04$	$-0.01 \pm 0.04$			$0.10 \pm 0.04$	$-0.02 \pm 0.06$
	N660	$-0.04 \pm 0.04$	$0.22 (0.09^a) \pm 0.04$	$-0.03 \pm 0.04$	$0.24 (0.11^a) \pm 0.04$			$-0.05 \pm 0.04$	

<sup>a</sup>Errors are for QM/MM and MM values are  $\pm$  standard deviations from 20 snapshots. Errors for X-ray distances are estimated from coordinate errors of hydrogen bonding atoms (Table SS). Errors for NMR-derived distances are estimated from the empirical fit used to convert chemical shifts to distances (Text S1). <sup>b</sup>Changes in hydrogen bond lengths are calculated relative to the corresponding distance in WT for each method. <sup>c</sup>Distance corrected by 0.13 Å for comparison of N·O to O·O hydrogen bond distances (Text S3).

3). However, in all other cases, which have shorter hydrogen bonds, the MM and QM/MM simulations predicted hydrogen bonds were longer than observed in the X-ray crystal structure models, with QM/MM generally providing closer agreement than MM (Figure S16, Table 3). For example, in the case of WT pKSI·DNP, MM predicts a Tyr16·DNP hydrogen bond length of 2.64  $\pm$  0.03 Å, whereas QM/MM predicts a value of  $2.55 \pm 0.02$  Å, closer to the length of  $2.50 \pm 0.02$  Å observed in the X-ray crystal structure. Additionally, in WT pKSI·DNP, MM and QM/MM predict Asp103·DNP hydrogen bond lengths of 2.60  $\pm$  0.02 and 2.59  $\pm$  0.03 Å, respectively, longer than the  $2.52 \pm 0.02$  Å distance in the X-ray crystal structure (Table 3).

#### CONCLUSIONS AND IMPLICATIONS

Since their initial description in the early 20th century, hydrogen bonds have been regarded as fundamental interactions in chemistry and biology. Despite their prevalence and importance, the observed diversity in hydrogen bond structure, with lengths that commonly vary from ~2.4 to 3.0 Å and angles from ~130 to 180°, has complicated our understanding of these interactions.<sup>53</sup> Indeed, Hopfinger concluded in 1973 that "The one definite fact about hydrogen bonds is that there does not appear to be any definite rules which govern their geometry". 123 Nevertheless, recent work 70 and the findings herein lead to a simpler view and a predictive model for hydrogen bond structure, where hydrogen bond lengths are primarily determined by the electronic properties of the donor/acceptor pair, irrespective of surroundings, and further secondarily affected by coupling within hydrogen bond networks. 124,125 Hydrogen bond lengths will also likely be influenced by other interactions not investigated here. Such an effect is exemplified by a 0.9 Å resolution X-ray structure of a thermostabilized mutant of carbonic anhydrase (PDB 6B00), where a hydrogen bond between the side chain of His94 and the carbonyl of Gln92 is 2.79 Å, which is 0.14 Å shorter than expected from the linear relationship between hydrogen bond length and  $\Delta p K_a$  (Figure 1A). A bound zinc is positioned such that it can polarize His94, presumably resulting in the shorterthan-predicted His94·Gln82 hydrogen bond.

Toward a Predictive Model for Hydrogen Bond Coupling. Sigala et al. observed that O·O hydrogen bond lengths in small molecules vary linearly with the  $\Delta p K_a$  of the hydrogen bond donor and acceptor molecules, with a slope of 0.02 Å/p $K_a$  (Figures 1A,B). 70,85,90 This dependence was common across environments, including organic and aqueous solutions and in crystals, and the same relationship was followed by proteins in aqueous solution and in crystals. The difference in proton affinity between the hydrogen bond donor and acceptor in aqueous solution provides a stand-in for donor and acceptor electronic properties<sup>79</sup> and accounts for ~86% of the variance seen in hydrogen bond lengths (Figure 1A). Nevertheless, there is still variation up to 0.17 Å in the case of 3,5-dinitrosalicylate, substantially exceeding experimental error (Figure 1C). $^{70}$  Here we showed, using the defined context of three different protein active sites, hydrogen bond coupling as an additional determinant of hydrogen bond structure, influencing hydrogen bond lengths in these systems by nearly 0.1 Å (Figure 9 and Table 1). This coupling is on the order of the variation in hydrogen bond lengths seen in crystals of 3,5-dinitrosalicylate (Figure 1C), and may cause much of the variation in lengths as these crystals exhibit diverse

hydrogen bonding patterns, and additional variation may arise from coordinating counterions (Figure S4).

Over a total of 19 measurements, using both <sup>1</sup>H NMR and high-resolution X-ray crystallography, we found a uniform coupling correlation where the change in secondary hydrogen bond length is  $-0.30 \pm 0.03$ -fold the change in the primary (Figure 9). This coupling was remarkably quantitatively similar in the three proteins used herein, despite different surroundings. In QM/MM simulations of pKSI, the oxyanion hole hydrogen bond lengths converged when the entire hydrogen bond network was included in the QM region (i.e., the side chains in Figure 2A), but were minimally influenced by the addition of another 898 atoms (Figure 10). Similarly, mutation of an arginine residue that is near to, but not involved in the PYP oxyanion hole hydrogen bond network, had no effect on oxyanion hole hydrogen bond lengths (Figure S13). These experimental and computational results suggest that hydrogen bond coupling is minimally influenced by residues not directly involved in the hydrogen bond networks and suggests that quantitative and predictive models can be made from the properties of the hydrogen bond donors and acceptors, along with the groups linked to the donor and acceptor within a hydrogen bond network.

Our current model for predicting hydrogen bond lengths is based primarily on the difference in donor and acceptor  $pK_a$ (Figure 1A,B) $^{70}$  and secondarily on the presence or absence of additional network hydrogen bonds, which presumably influence the donor and acceptor electronic properties (Figure 9 and Table 1).84,85 Our results show that QM/MM, but not MM models, can reasonably predict the coupling effects for extended hydrogen bond networks suggesting that polarization effects are propagated, though highly damped, through these networks. This model holds for condensed-phase environments and has been quantum mechanically tested over a dielectric range of 5-80,  $^{70}$  but we anticipate that there will be larger and less predictable effects in the gas phase, due to the undamped electrostatic forces that can extend over longer distances.

These data can also be used to derive empirical predictions. Hydrogen bond lengths and changes in these lengths observed in X-ray and computational structural models can be compared to our empirical scale to identify potential errors or unique cases. Anecdotally, we have identified hydrogen bonds in the Protein Data Bank that deviate significantly from predicted lengths, based on the  $\Delta pK_s$  correlation (Figure 1A). For the cases examined, the distances cannot be considered reliable because the single-conformation structures deposited do not account for the multiple conformations of the hydrogen bond donor and/or acceptor that are suggested by the electron density maps (J. Fraser, personal communication).

In the future, comparing hydrogen bond lengths derived from computational models to those predicted empirically may provide an additional means to evaluate computational models, and the potential accuracy of additional conclusions derived from these models.

Hydrogen Bond Networks and Enzyme Dynamics. Here we have evaluated static coupling of hydrogen bond lengths within a network. The relationship revealed may also be applicable to dynamic processes and aid in our understanding of temporally coupled motions within proteins. Oxyanion holes are common in enzyme active sites where they donate hydrogen bonds to stabilize the growing charge on the transition state. A simple prediction from our model is that

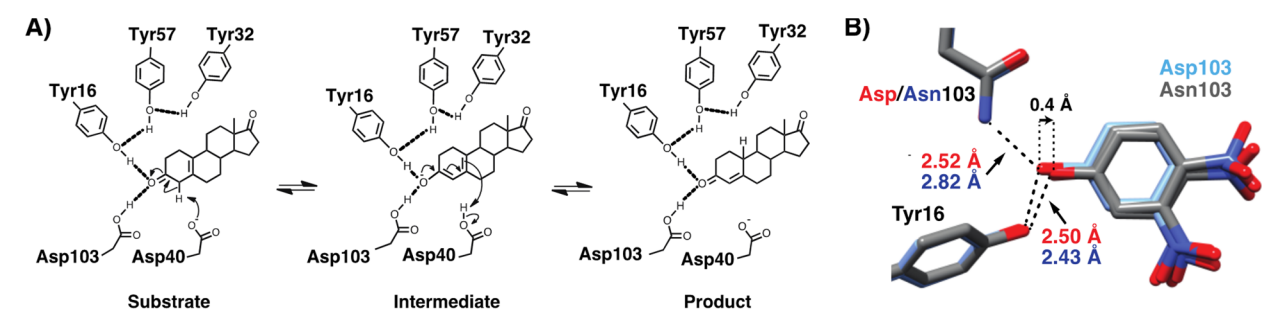


Figure 12. Possible coupled changes in hydrogen bond lengths along the reaction coordinate. (A) Mechanism of Isomerization of 5(10)-estrene-3,17-dione by KSI. Bond lengths that are predicted to shorten or lengthen are shown in red and cyan, respectively. (B) Global alignments of pKSI-DNP (1.10 Å) and pKSI D103N·DNP (1.05 Å) indicate a 0.4 Å shift in the position of DNP oxyanion. This shift is larger than the coordinate errors in these structures (Table S4).

oxyanion hole hydrogen bonds shorten in the transition state relative to the ground state of the reaction. For example, KSI catalyzes the isomerization of double bonds in steroid substrates in a two-step mechanism where the general base first abstracts a proton from the substrate, forming a dienolate intermediate, followed by the addition of a proton at a different steroid position, to form the isomerized product (Figure 12A). The difference in  $pK_a$  going from the ground state carbonyl oxygen to the dienolate intermediate is ~16 units, <sup>126</sup> leading to a predicted shortening of the oxyanion hole hydrogen bonds by ~0.32 Å, which is presumably accompanied by alterations in the lengths of the other network hydrogen bonds (Figure 12A). In addition to these changes, the reduction of carbonoxygen bond order from the ground state carbonyl to the intermediate dienolate lengthens the substrate carbon—oxygen bond.

As an initial modest step toward understanding coupling, we compared the high-resolution crystal structures of pKSI·DNP and pKSI Asp103Asn·DNP determined herein and found that most of the structural differences arise from movement of the bound ligand, DNP, which shifts "backward" in the active site by 0.4 Å and toward Tyr16 to accommodate the longer Asp103Asn hydrogen bond (Figure 12B). This suggests that substrates may be more mobile than the enzyme groups in the reaction cycle, although these hydrogen bond rearrangements and movements will be altered by the additional constraint of the concerted proton transfer. An experimental and computational model of expected differences in hydrogen bond lengths between a substrate and intermediate may help identify candidate groups that are dynamically coupled along the reaction coordinate and may aid in unraveling and understanding active site and protein dynamics.

Though the hydrogen bond network perturbations made herein result in measurable changes in the oxyanion hole hydrogen bond lengths (Table 1), the functional effects from the mutations responsible for these changes are small. For example, in pKSI the Asp103Asn mutation, which results in a 0.30 Å lengthening of the Asp/Asn103·DNP hydrogen bond (0.17 Å corrected for comparison of O·O to N·O hydrogen bonds) results in a 13-fold decrease in  $k_{\rm cat}$ . Even smaller changes in  $k_{\rm cat}$ , of <2-fold, are observed upon replacement of Tyr16 with fluoro-tyrosine residues. These small functional effects are consistent with shallow hydrogen bond energetics in the KSI active site, 90,95 and our ability to now relate structural perturbations to catalytic effects may help further evaluate energetic models for enzyme catalysis.

#### MATERIALS AND METHODS

A detailed description of the experimental and computational methods can be found in the Supporting Information. 3,5-Dinitrosalicylate hydrogen bond lengths were collated from the Cambridge Structural Database. KSI and PYP were expressed and purified as previously described. S5,128 KSI semisynthesis was conducted as previously described with one difference, as detailed in the Supporting Information. H NMR spectra of KSI and PYP were acquired at the Stanford Magnetic Resonance Laboratory on an 800 MHz Varian UNITYINOVA spectrometer at  $-3.3\pm0.2\,^{\circ}\mathrm{C}$  using a 1331 binomial pulse sequence with samples consisting of 0.4–1.0 mM KSI or PYP and 1.0–5.0 mM ligand in 40 mM potassium phosphate (pH 7.2), 1 mM sodium·EDTA, 2 mM DTT and 10% DMSO- $d_6$  (v/v). Single crystal diffraction data was collected at Stanford Synchrotron Radiation Light Source and processed as described in the Supporting Information. Detailed descriptions of MM and QM/MM simulations can be found in the Supporting Information.

#### ASSOCIATED CONTENT

# Supporting Information

The Supporting Information is available free of charge on the ACS Publications website at DOI: 10.1021/jacs.8b01596.

Data for 6C1X (CIF)

Data for 6c1x (CIF)

Data for 6C1J (CIF)

Data for 6c1j (CIF)

Data for 6C17 (CIF)

Data for 6c17 (CIF)

Additional discussion on the conversion of <sup>1</sup>H NMR chemical shifts to hydrogen bond distances, data and analysis of the ionization states of ligands bound to F-Tyr variants, analysis and discussion of the correction for longer N·O versus O·O hydrogen bonds, crystallographic data collection and refinement statistics for pKSI structures determined herein, as well as additional clarifying figures and tables (PDF)

# AUTHOR INFORMATION

# **Corresponding Author**

\*herschla@stanford.edu

#### ORCID ®

Margaux M. Pinney: 0000-0002-7735-5032

Fang Liu: 0000-0003-1322-4997 Ruibin Liang: 0000-0001-8741-1520 Todd J. Martinez: 0000-0002-4798-8947 Daniel Herschlag: 0000-0002-4685-1973

#### **Present Addresses**

<sup>¶</sup>Department of Chemical Engineering, Massachusetts Institute of Technology, Cambridge, MA 02139, USA

<sup>V</sup>Department of Chemistry and Biochemistry, California State University Long Beach, Long Beach, CA 90840, USA

#### Notes

The authors declare no competing financial interest.

#### ACKNOWLEDGMENTS

This work was funded by a National Science Foundation (NSF) Grant (MCB-1714723). M.M.P. and D.M.S. were supported by NSF Graduate Research Fellowships. A.N. was supported, in part, by an HHMI International Student Research Fellowship, an NSERC Postgraduate Scholarship and a William and Sara Hart Kimball Stanford Graduate Fellowship. F.Y. was supported by a Human Frontiers Postdoctoral Fellowship. F.L. was partially supported by an Evelyn Laing McBain Fellowship. We would like to thank Dr. Corey W. Liu, Stanford Magnetic Resonance Laboratory, for assistance with NMR spectroscopy. The SMRL 800 MHz NMR was supported in part by NIH Shared Instrumentation Grant 1 S10 RR025612-01A1. We also thank S. Alvarez for analysis of O·O and N·O hydrogen bond lengths in the Cambridge Structural Database, J. Fraser for investigation of hydrogen bond lengths in ultrahigh resolution crystal structures from the PDB, P. Sigala and R. Parrish for helpful comments and discussions, and members of the Herschlag lab for comments on the paper and stimulating discussions.

# **■** REFERENCES

- (1) Pauling, L. J. Am. Chem. Soc. 1931, 53, 1367-1400.
- (2) "It has been recognized that hydrogen bonds restrain protein molecules to their native configurations, and I believe that as the methods of structural chemistry are further applied to physiological problems it will be found that the significance of the hydrogen bond for physiology is greater than that of any other single structural feature." -Linus Pauling, Nature of the Chemical Bond and the Structure of Molecules and Crystals (1939), p 265.
- (3) Jeffrey, G. A.; Saenger, W. Hydrogen Bonding in Biological Structures; Springer: Berlin, Germany, 1991.
- (4) Fersht, A. R. Trends Biochem. Sci. 1987, 12, 301-304.
- (5) Williams, M. A.; Ladbury, J. E. Hydrogen Bonds in Protein-Ligand Complexes. In Protein-Ligand Interactions: From Molecular Recognition to Drug Design; Schneider, H.-J. B. a. G., Ed.; Wiley-VCH Verlag GmbH & Co. KGaA: Weinheim, Germany, 2003; pp 137-
- (6) Perrin, C. L.; Nielson, J. B. Annu. Rev. Phys. Chem. 1997, 48, 511 - 544.
- (7) Shan, S. O.; Herschlag, D. Methods Enzymol. 1999, 308, 246-276.
- (8) Judd, E. T.; Stein, N.; Pacheco, A. A.; Elliott, S. J. Biochemistry **2014**, *53* (35), *5638*–*5646*.
- (9) Sanchez-Azqueta, A.; Herguedas, B.; Hurtado-Guerrero, R.; Hervas, M.; Navarro, J. A.; Martinez-Julvez, M.; Medina, M. Biochim. Biophys. Acta, Bioenerg. 2014, 1837 (2), 251-263.
- (10) Xu, D.; Tsai, C. J.; Nussinov, R. Protein Eng., Des. Sel. 1997, 10, 999-1012.
- (11) Rose, G. D.; Wolfenden, R. Annu. Rev. Biophys. Biomol. Struct. **1993**, 22, 381–415.
- (12) Bolen, W. D.; Rose, G. D. Annu. Rev. Biochem. 2008, 77 (1), 339-362.
- (13) Wells, J. A.; Cunningham, B. C.; Graycar, T. P.; Estell, D. A. Philos. Trans. R. Soc., A 1986, 317, 415-423.
- (14) Cui, Q.; Karplus, M. Protein Sci. 2008, 17 (8), 1295-1307.

- (15) Gardino, A. K.; Villali, J.; Kivenson, A.; Lei, M.; Liu, C.; Steindel, P.; Eisenmesser, E. Z.; Labeikovsky, W.; Wolf-Watz, M.; Clarkson, M. W.; Kern, D. Cell 2009, 139 (6), 1109-1118.
- (16) Kiss, G.; Çelebi-Ölçüm, N.; Moretti, R.; Baker, D.; Houk, K. N. Angew. Chem., Int. Ed. 2013, 52 (22), 5700-5725.
- (17) Chakrabarti, R.; Klibanov, A. M.; Friesner, R. A. Proc. Natl. Acad. Sci. U. S. A. 2005, 102 (34), 12035-12040.
- (18) Kortemme, T.; Joachimiak, L. A.; Bullock, A. N.; Schuler, A. D.; Stoddard, B. L.; Baker, D. Nat. Struct. Mol. Biol. 2004, 11 (4), 371-
- (19) Joachimiak, L. A.; Kortemme, T.; Stoddard, B. L.; Baker, D. J. Mol. Biol. 2006, 361 (1), 195-208.
- (20) Stranges, P. B.; Kuhlman, B. Protein Sci. 2013, 22 (1), 74-82.
- (21) Sheinerman, F. B.; Honig, B. J. Mol. Biol. 2002, 318 (1), 161-177.
- (22) Pauling, L. Chem. Eng. News 1946, 24 (10), 1375-1377.
- (23) Benkovic, S. J.; Hammes-Schiffer, S. Science 2003, 301, 1196-
- (24) Cannon, W. R.; Singleton, S. F.; Benkovic, S. J. Nat. Struct. Mol. Biol. 1996, 3 (10), 821-833.
- (25) Fersht, A. R. Structure and Mechanism in Protein Science; Freeman: New York, NY, 1999.
- (26) Ustinov, A.; Weissman, H.; Shirman, E.; Pinkas, I.; Zuo, X.; Rybtchinski, B. J. Am. Chem. Soc. 2011, 133 (40), 16201-16211.
- (27) Freire, E. Annu. Rev. Biophys. Biomol. Struct. 1995, 24, 141-165.
- (28) Betz, S. F.; Raleigh, D. P.; DeGrado, W. F. Curr. Opin. Struct. Biol. 1993, 3 (4), 601-610.
- (29) DeGrado, W. F.; Raleigh, D. P.; Handel, T. Curr. Opin. Struct. Biol. 1991, 1 (6), 984-993.
- (30) Klinman, J. P. Biochemistry 2013, 52 (12), 2068-2077.
- (31) Klinman, J. P.; Kohen, A. Annu. Rev. Biochem. 2013, 82, 471-
- (32) Hammes-Schiffer, S.; Benkovic, S. J. Annu. Rev. Biochem. 2006, 75, 519-541.
- (33) Boehr, D. D.; McElheny, D.; Dyson, H. J.; Wright, P. E. Science 2006, 313 (5793), 1638-1642.
- (34) Adamczyk, A. J.; Cao, J.; Kamerlin, S. C. L.; Warshel, A. Proc. Natl. Acad. Sci. U. S. A. 2011, 108 (34), 14115-14120.
- (35) Loveridge, E. J.; Tey, L. H. H.; Behiry, E. M.; Dawson, W. M.; Evans, R. M.; Whittaker, S. B.; Günther, U. L.; Williams, C.; Crump, M. P.; Allemann, R. K. J. Am. Chem. Soc. 2011, 133 (50), 20561-
- (36) Luk, L. Y. P.; Ruiz-Pernía, J. J.; Dawson, W. M.; Roca, M.; Loveridge, E. J.; Glowacki, D. R.; Harvey, J. N.; Mulholland, A. J.; Tuñón, I.; Moliner, V.; Allemann, R. K. Proc. Natl. Acad. Sci. U. S. A. 2013, 110 (41), 16344-16349.
- (37) Schramm, V. L. Annu. Rev. Biochem. 2011, 80 (1), 703-732.
- (38) Kohen, A.; Cannio, R.; Bartolucci, S.; Klinman, J. P. Nature **1999**, 399 (6735), 496-499.
- (39) Klinman, J. P. Acc. Chem. Res. 2015, 48 (2), 449-456.
- (40) Nagel, Z. D.; Dong, M.; Bahnson, B. J.; Klinman, J. P. Proc. Natl. Acad. Sci. U. S. A. 2011, 108 (26), 10520-10525.
- (41) Nagel, Z. D.; Cun, S.; Klinman, J. P. J. Biol. Chem. 2013, 288 (20), 14087-14097.
- (42) Meadows, C. W.; Ou, R.; Klinman, J. P. J. Phys. Chem. B 2014, 118 (23), 6049-6061.
- (43) Liang, Z. X.; Klinman, J. P. Curr. Opin. Struct. Biol. 2004, 14 (6), 648-655.
- (44) Herschlag, D.; Natarajan, A. Biochemistry 2013, 52 (12), 2050-
- (45) Offenbacher, A. R.; Hu, S.; Poss, E. M.; Carr, C. A. M.; Scouras, A. D.; Prigozhin, D. M.; Iavarone, A. T.; Palla, A.; Alber, T.; Fraser, J. S.; Klinman, J. P. ACS Cent. Sci. 2017, 3, 570-579.
- (46) Fleming, P. J.; Rose, G. D. Protein Sci. 2005, 14 (7), 1911-1917.
- (47) Kityk, R.; Vogel, M.; Schlecht, R.; Bukau, B.; Mayer, M. P. Nat. *Commun.* **2015**, *6*, 1–11.
- (48) Li, G. C.; Srivastava, A. K.; Kim, J.; Taylor, S. S.; Veglia, G. Biochemistry 2015, 54 (26), 4042-4049.

- (49) Zimanyi, C. M.; Chen, P. Y.; Kang, G.; Funk, M. A.; Drennan, C. L. eLife **2016**, *5*, e07141.
- (50) We address dynamics in hydrogen bond networks by investigating how changes in hydrogen bond lengths at equilibrium are propagated to other network hydrogen bonds. Temporal coupling is expected, but is more difficult to probe unambiguously by experiment.
- (51) Gilli, G.; Gilli, P. The Nature of the Hydrogen Bond: Outline of a Comprehensive Hydrogen Bond Theory; Oxford University Press Inc.: New York, NY, 2009.
- (52) Jeffrey, G. A. Crystallogr. Rev. 1995, 4 (3), 213-254.
- (53) Jeffrey, J. A. An Introduction to Hydrogen Bonding; Oxford University Press: Oxford, U. K., 1997.
- (54) Pimental, G. C.; McClellan, A. L. *The Hydrogen Bond*; W. H. Freeman and Company: San Francisco, CA, 1960.
- (55) Steiner, T. Angew. Chem., Int. Ed. 2002, 41, 48-76.
- (56) Meot-Ner, M. Chem. Rev. 2005, 105 (1), 213-284.
- (57) Kreevoy, M. M.; Liang, T. J. Am. Chem. Soc. 1980, 102 (10), 3315–3322.
- (58) Gerlt, J. A.; Kreevoy, M. M.; Cleland, W. W.; Frey, P. A. *Chem. Biol.* **1997**, *4* (4), 259–267.
- (59) Cleland, W.; Kreevoy, M. Science 1994, 264 (5167), 1887–1890.
- (60) Bowie, J. U. Curr. Opin. Struct. Biol. 2011, 21 (1), 42-49.
- (61) Gao, J.; Bosco, D. A.; Powers, E. T.; Kelly, J. W. Nat. Struct. Mol. Biol. 2009, 16 (7), 684–690.
- (62) Warshel, A.; Papazyan, A. Proc. Natl. Acad. Sci. U. S. A. 1996, 93 (24), 13665–13670.
- (63) Feierberg, I.; Aqvist, J. Biochemistry 2002, 41, 15728-15735.
- (64) Lin, I. J.; Gebel, E. B.; Machonkin, T. E.; Westler, W. M.; Markley, J. L. *Proc. Natl. Acad. Sci. U. S. A.* **2005**, *102* (41), 14581–14586.
- (65) Perrin, C. L. Science 1994, 266 (5191), 1665-1668.
- (66) Mildvan, A. S.; Harris, T. K.; Abeygunawardana, C. Methods Enzymol. 1999, 308, 219-245.
- (67) Hibbert, F.; Emsley, J. Adv. Phys. Org. Chem. 1991, 26, 255-379.
- (68) Herschlag, D.; Pinney, M. M. Biochemistry 2018, 57, 3338.
- (69) See ref 68 for a further discussion on hydrogen bond structure and energetics.
- (70) Sigala, P. A.; Ruben, E. A.; Liu, C. W.; Piccoli, P. M. B.; Hohenstein, E. G.; Martínez, T. J.; Schultz, A. J.; Herschlag, D. *J. Am. Chem. Soc.* **2015**, *137* (17), 5730–5740.
- (71) Chen, J.; McAllister, M.; Lee, J. K.; Houk, K. N. J. Org. Chem. 1998, 63, 4611–4619.
- (72) Schwartz, B.; Drueckhammer, D. G.; Usher, K. C.; Remington, S. J. *Biochemistry* **1995**, 34, 15459–15466.
- (73) Frey, P. A.; Whitt, S. A.; Tobin, J. B. Science 1994, 264, 1927–1930.
- (74) Garcia-Viloca, M.; González-Lafont, A.; Lluch, J. M. J. Phys. Chem. A 1997, 101, 3880-3886.
- (75) Remer, L. C.; Jensen, J. H. J. Phys. Chem. A **2000**, 104 (40), 9266–9275.
- (76) Gilli, P.; Pretto, L.; Bertolasi, V.; Gilli, G. Acc. Chem. Res. 2009, 42 (1), 33-44.
- (77) The difference in  $pK_a$  between the hydrogen bond donor and acceptor acts as a proxy for differences in the electronic properties of these groups, which determines the length of the hydrogen bond. See references Gross, et. al (2001) and Charton, et al. (2007).
- (78) Charton, M. *Prog. Phys. Org. Chem.*; John Wiley & Sons, Inc.: Hoboken, NJ, 2007; Vol. 13, pp 119–251.
- (79) Gross, K. C.; Seybold, P. G. Int. J. Quantum Chem. **2001**, 85 (4–5), 569–579.
- (80) Allen, F. H. Acta Crystallogr., Sect. B: Struct. Sci. 2002, 58 (3), 380–388.
- (81) Allen, F. H.; Cole, J. C.; Howard, J. A. K. Acta Crystallogr., Sect. A: Found. Crystallogr. 1995, 51 (2), 95–111.
- (82) Allen, F. H.; Cole, J. C.; Howard, J. A. K. Acta Crystallogr., Sect. A: Found. Crystallogr. 1995, 51, 112–121.

- (83) This phenomenon, also also referred to as "crystal-field effects", has been previously discussed in the literature and remains elusive. See Jeffrey (1995).
- (84) Sigala, P. A.; Caaveiro, J. M. M.; Ringe, D.; Petsko, G. A.; Herschlag, D. *Biochemistry* **2009**, 48 (29), 6932–6939.
- (85) Sigala, P. A.; Tsuchida, M. A.; Herschlag, D. Proc. Natl. Acad. Sci. U. S. A. 2009, 106 (23), 9232–9237.
- (86) Tolstoy, P. M.; Schah-Mohammedi, P.; Smirnov, S. N.; Golubev, N.; Denisov, G. S.; Limbach, H. H. J. Am. Chem. Soc. 2004, 126, 5621–5634.
- (87) Bolvig, S.; Hansen, P. E. Curr. Org. Chem. 2000, 4, 19-54.
- (88) Detering, C.; Tolstoy, P. M.; Golubev, N. S.; Denisov, G. S.; Limbach, H. H. Dokl. Phys. Chem. 2001, 379, 191–193.
- (89) Altman, L. J.; Laungani, D.; Gunnarsson, G.; Wennerstrom, H.; Forsen, S. J. Am. Chem. Soc. 1978, 100, 8264–8266.
- (90) Kraut, D. A.; Sigala, P. A.; Pybus, B.; Liu, C. W.; Ringe, D.; Petsko, G. A.; Herschlag, D. *PLoS Biol.* **2006**, *4* (4), e99.
- (91) Borgstahl, G. E. O.; Williams, D. R.; Getzoff, E. D. Biochemistry 1995, 34, 6278-6287.
- (92) Imamoto, Y.; Kataoka, M. Photochem. Photobiol. 2007, 83 (1), 40-49.
- (93) Childs, W.; Boxer, S. G. Biochemistry 2010, 49 (12), 2725-2731.
- (94) Petrounia, I.; Pollack, R. M. Biochemistry 1998, 37, 700-705.
- (95) Natarajan, A.; Schwans, J. P.; Herschlag, D. J. Am. Chem. Soc. **2014**, 136 (21), 7643–7654.
- (96) Jeffrey, G. A.; Yeon, Y. Acta Crystallogr., Sect. B: Struct. Sci. 1986, 42, 410-413.
- (97) Mildvan, A. S.; Harris, T. K.; Abeygunawardana, C. Methods in Enzymology; Academic Press: New York, NY, 1999; Vol. 308, pp 219–245.
- (98) Harris, T. K.; Mildvan, A. S. Proteins: Struct., Funct., Genet. 1999, 35 (3), 275-282.
- (99) McDermott, A.; Ridenour, C. F. Encyclopedia of NMR; Wiley: Sussex, U. K., 1996.
- (100) Harris, T. K.; Zhao, Q.; Mildvan, A. S. J. Mol. Struct. 2000, 552, 97–109.
- (101) Harris, T. K.; Abeygunawardana, C.; Mildvan, A. S. Biochemistry 1997, 36, 14661–14675.
- (102) Agarwal, V.; Linser, R.; Fink, U.; Faelber, K.; Reif, B. J. Am. Chem. Soc. 2010, 132, 3187–3195.
- (103) Guo, J.; Koeppe, B.; Tolstoy, P. M. Phys. Chem. Chem. Phys. **2011**, *13*, 2335–2341.
- (104) Marks, G. T.; Harris, T. K.; Massiah, M. A.; Mildvan, A. S.; Harrison, D. H. T. *Biochemistry* **2001**, *40*, 6805–6818.
- (105) Sun, Y.; Yin, S.; Feng, Y.; Li, J.; Zhou, J.; Liu, C.; Zhu, G.; Guo, Z. J. Biol. Chem. **2014**, 289, 15867–15879.
- (106) Tolstoy, P. M.; Schah-Mohammedi, P.; Smirnov, S. N.; Golubev, N.; Denisov, G. S.; Limbach, H. H. *J. Am. Chem. Soc.* **2004**, *126*, 5621–5634.
- (107) Steiner, T.; Saenger, W. Acta Crystallogr., Sect. B: Struct. Sci. 1994, 50, 348–357.
- (108) Sigala, P. A.; Fafarman, A. T.; Schwans, J. P.; Fried, S. D.; Fenn, T. D.; Caaveiro, J. M. M.; Pybus, B.; Ringe, D.; Petsko, G. A.; Boxer, S. G.; Herschlag, D. *Proc. Natl. Acad. Sci. U. S. A.* **2013**, *110* (28), E2552–E2561.
- (109) As noted above, the two oxyanion hole hydrogen bonds are clearly resolved with other ligands bound (Figure S5,6), and though prior data support these assignments, reversing the assignment would not significantly affect our conclusions.
- (110) Alvarez, S. Dalton Trans. 2013, 42, 8617-8636.
- (111) Sugishima, M.; Tanimoto, N.; Soda, K.; Hamada, N.; Tokunaga, F.; Fukuyama, K. Acta Crystallogr., Sect. D: Biol. Crystallogr. **2004**, *60*, 2305–2309.
- (112) Yamaguchi, S.; Kamikubo, H.; Kurihara, K.; Kuroki, R.; Niimura, N.; Shimizu, N.; Yamazaki, Y.; Kataoka, M. *Proc. Natl. Acad. Sci. U. S. A.* **2009**, *106*, 440–444.

- (113) Kim, D.-H.; Jang, D. S.; Nam, G. H.; Choi, G.; Kim, J.-S.; Ha, N.-C.; Kim, M.-S.; Oh, B.-H.; Choi, K. Y. *Biochemistry* **2000**, *39*, 4581–4589.
- (114) Dwyer, D. S. BMC Chem. Biol. 2005, 5 (1), 1-11.
- (115) Kraut, D. A.; Carroll, K. S.; Herschlag, D. Annu. Rev. Biochem. **2003**, 72, 517–71.
- (116) As above, the Tyr57Phe mutant was made in the Tyr32Phe background to avoid known rearrangements in the single Tyr57Phe mutant.
- (117) We have collected 19 measurements of length changes in both oxyanion hole hydrogen bonds upon perturbation and 3 measurements of lengths changes in only one oxyanion hole hydrogen bond (see Table 1).
- (118) CRC Handbook of Chemistry and Physics, 83rd ed.; CRC Press: Boca Raton, FL, 2003.
- (119) Cohen, A. J.; Mori-Sánchez, P.; Yang, W. Science 2008, 321 (5890), 792-794.
- (120) Rudberg, E. J. Phys.: Condens. Matter 2012, 24, 072202.
- (121) Isborn, C. M.; Mar, B. D.; Curchod, B. F. E.; Tavernelli, I.; Martínez, T. J. *Phys. Chem. B* **2013**, *117* (40), 12189–12201.
- (122) Kulik, H. J.; Luehr, N.; Ufimtsev, I. S.; Martinez, T. J. J. Phys. Chem. B **2012**, 116 (41), 12501–12509.
- (123) Hopfinger, A. J. Conformation Properties of Macromolecules; Academic Press: New York, NY, 1973.
- (124) Herein we refer to equilibrium hydrogen bond lengths. However, O–H vibrational frequencies within O·O hydrogen bonds are sensitive to their surroundings (e.g., dielectric), as has been explored in detail using valence bond-based theoretical approaches. See Kiefer, et al. (2014).
- (125) Kiefer, P. M.; Pines, E.; Pines, D.; Hynes, J. T. J. Phys. Chem. B **2014**, 118 (28), 8330–8351.
- (126) Zeng, B.; Pollack, R. M. J. Am. Chem. Soc. 1991, 113, 3838-3842.
- (127) Lamba, V.; Yabukarski, F.; Pinney, M.; Herschlag, D. J. Am. Chem. Soc. 2016, 138 (31), 9902–9909.
- (128) Kraut, D. A.; Sigala, P. A.; Fenn, T. D.; Herschlag, D. Proc. Natl. Acad. Sci. U. S. A. 2010, 107 (5), 1960–1965.
- (129) Koeppe, B.; Tolstoy, P. M.; Limbach, H.-H. J. Am. Chem. Soc. **2011**, 133 (20), 7897–7908.
- (130) Jencks, W. P.; Regenstein, J. Handbook of Biochemistry and Molecular Biology; CRC Press: Cleveland, OH, 1976.
- (131) Thornburg, L. D.; Henot, F.; Bash, D. P.; Hawkinson, D. C.; Bartel, S. D.; Pollack, R. M. *Biochemistry* **1998**, *37*, 10499–10506.